Vienna University of Technology
Institute of Energy Systems and Electrical Drives

Master thesis

Analysis of passive LED drivers

Diplomarbeit

Analyse von passiven LED-Vorschaltgeräten

Author:
Daniel Andersen
Registration number
0928261

Supervisor:
Ao. Univ.Prof. Dipl.-Ing.
Dr.techn. Johann Ertl

March 2, 2014

Contents

Kurzfassung

Die vorliegende Diplomarbeit beschäftigt sich mit der Untersuchung von zwei einfachen passiven LED-Treibern zur Anwendung bei Straßenbeleuchtungen. Der Hintergrund der Arbeit liegt in der Tatsache, dass die untersuchten passiven LED-Treiber wegen ihrer Einfachheit, Robustheit und damit ihrer Zuverlässigkeit eine sehr lange Lebensdauer erwarten lassen. Vorausgegangene praktische Untersuchungen, welche am Institut für Energiesysteme und Elektrische Antriebe (ESEA) mit einem solchen LED-Treiber durchgeführt wurden, waren sehr vielversprechend. Die dieser Arbeit zugrunde liegende Idee ist es, die praktischen Versuche durch theoretische Überlegungen und analytische Berechnungen abzusichern. Als Ansatz für diese Berechnungen dient eine vereinfachte Ersatzschaltung, wobei alle ohmschen Bauteilkomponenten vernachlässigt werden. Danach erfolgt eine Verifizierung der LED- Treiber (ein- bzw. dreiphasige Variante) mit einem Schaltungssimulator-Programm (Pspice) simuliert, wobei die ohmschen Komponenten berücksichtigt werden. Die Ergebnisse der einzelnen Berechnungen, Simulationen und experimentellen Messungen werden verglichen und diskutiert. Die Ergebnisse zeigen, dass die vorgeschlagenen passiven Schaltungen unter bestimmten Betriebsbedingungen sehr gut zur Speisung von LED-Leuchten aus dem Ein- bzw. Dreiphasennetz verwendet werden können.

Abstract

This master thesis deals with the examination of two simple passive LED drivers minded for street light devices. The background for the interest of the presented passive LED drivers is their simplicity, robustness, and hence their reliability which result most likely in a very long useful lifetime. A practical experiment on one type of the LED drivers has been executed at the ESEA institute prior to this work. The idea with this thesis is to continue the research from a more theoretical point of view. The approach for the calculations is taken in a simplified equivalent circuit where the resistive parts are neglected. Thereafter, the circuits of the LED drivers with added resistance parts are simulated numerically using Pspice. The results from the calculations, simulations, and the experimental measurements are compared and discussed. The results show that LED units under specific operating parameters very well can be operated by using simple passive driver stages.

Acknowledgement

I here want to express my gratitude to my supervisor Univ. Prof. Dipl.-Ing. Dr.techn. Johann Ertl for his support and for letting me finish this work abroad. The at all time fast response from your side have been highly appreciated.

Further I want to thank my wife for her assistance during this work, especially for encouraging me and discussing the development of my thesis with me. Last but not least, I want to say thank you to my father in law for his corrections and his feedback.

1 Introduction

1.1 Motivation

LEDs have become more and more present in our everyday live. The light emitting diode can be found in many electrical devices we use or which surround us. The LED is different from other light sources because it is a semiconductor light source. Remarkable advantages lay in the efficiency and lifetime expectations if compared with other light sources. Some LED manufacturers predict lifetimes up to 100.000 hours if the LED is operated under the right conditions. Yet, a disadvantage in using LEDs is that they cannot be connected directly to the main public alternating grid. Only an appropriated direct current in forward direction of the LED makes it glow. A switched mode power supply (SMPS) is usually used within the light application to make the connection between the power grid and the LEDs. SMPS used for LEDs are commonly referred to as LED drivers. The SMPS guarantees that the LEDs are supplied with the right direct current for operation. SMPS are today produced in droves all around the world and have become the standard part in many different electrical devices which need an internal direct current. Examples of devices that contain SMPS are computers, radios, televisions etc. An SMPS is an active power supply which allows the supply voltage to vary in amplitude and frequency. This feature makes the device less sensitive to disturbances in the connected supply voltage and offers the possibility to connect the device to the available local supply voltage almost all around the world. One of the disadvantages using SMPS is the complexity of the circuits. Despite the diversity of the different types of SMPS, the circuits generally require a controller IC, one or more power transistors, diodes, inductors and capacitors.
However, the idea with this master thesis is to analyze two simple passive LED drivers supplying a LED street light device. In this thesis a single and a three-phase passive LED driver are analyzed and discussed. The suggested passive drivers only consist of rectifier and inductors and need no other electrical parts for operation. The reason why street light devices are chosen for this research is not picked randomly. The major argument for this is the fact that life span plays an important role due to the circumstantial maintenance of street lights.

1.2 Focus and Aim

The key aspect in this master thesis is to find out the usability and functioning of the suggested passive LED drivers from an electrical point of view. Experimental tests of the single phase circuit have been executed at the institute ESEA already in 2012. The test report is to be found in appendix section D. The experiment was executed successfully and has shown positive results. This thesis is continues the experimental test from a more theoretical point of view. The intention is to determine the usability and functioning from a strictly theoretical perspective, by means of calculations and simulation. The aim is to constitute relevant parameters and to find out under what possible conditions the circuit can be operated theoretically. In section 2.3 some statements on lifetime expectations for the used components are added. What is especially interesting in the presented circuits is their simplicity and robustness, as the following argumentation demonstrates. A full lifetime analysis of the circuits in section 2.2 will not be part of this thesis, nor will the design of the used inductors be presented in this work. Instead, the appropriate electrical size, measured in Henry, will be specified.

2 Background information

2.1 System

The two passive LED drivers which will be analyzed in this report are a single-phase and a three-phase driver. Characteristic of both drivers is that the supply voltage is meant to come from an AC source of adjustable amplitude. Further the adjustable source for the drivers is supplied from the main public grid. The main public grid is understood as a 3-phase system with 50Hz and 230V phase-to-neutral and 400V phase-to-phase voltage within a dedicated tolerance band. The structure of how the supply voltage for the LED drivers is connected is pictured in figure 2.1 and 2.2. The frequency before and after the adjustable supply source for the drivers is identical. However, the adjustable supply source is only then supposed to lower the supply voltage for the LED lamps below the voltage from the main grid, when a dimming effect is required. How this supply source is designed shall not be discussed further in this report. What is important however is the fact that the supply source is supposed to be placed externally from the LED light application itself. The idea is to create a common separate alternating supply grid only for the LED street lights with a dimming effect at sun set and sun rise.

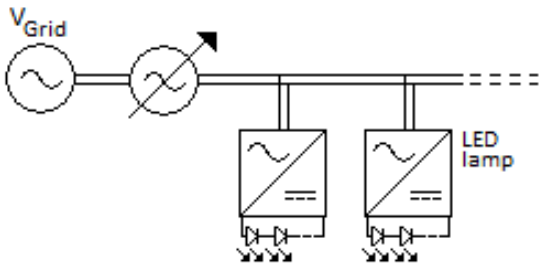

Figure 2.1: Overview LED driver connection to grid single-phase system

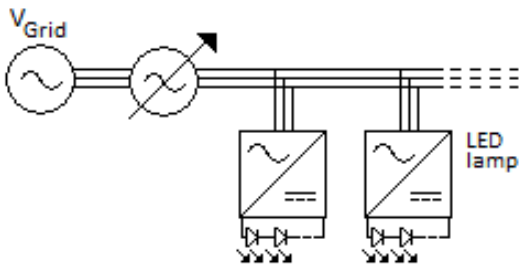

Figure 2.2: Overview LED driver connection to grid three-phase system

2.2 LED drivers

The LED driver for the single-phase system consists of a simple B2-Bridge combined with an inductor. The bridge is also known as the single-phase full wave rectifier. The structure of the circuit is illustrated below in figure 2.3. The connection to the adjustable supply grid is done at the left inlet.

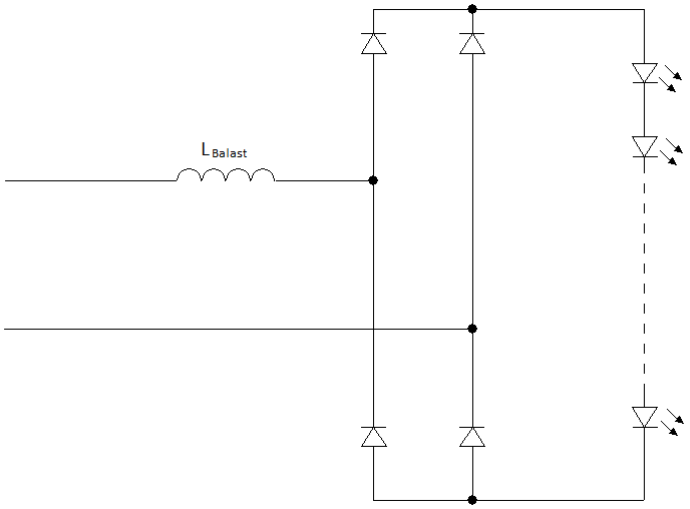

Figure 2.3: B2 single-phase LED driver

In figure 2.4 the structure of the three-phase LED driver is pictured. The represented circuit is the common six-pulse rectifier. The connection to the adjustable three-phase supply grid is done at the left inlet.

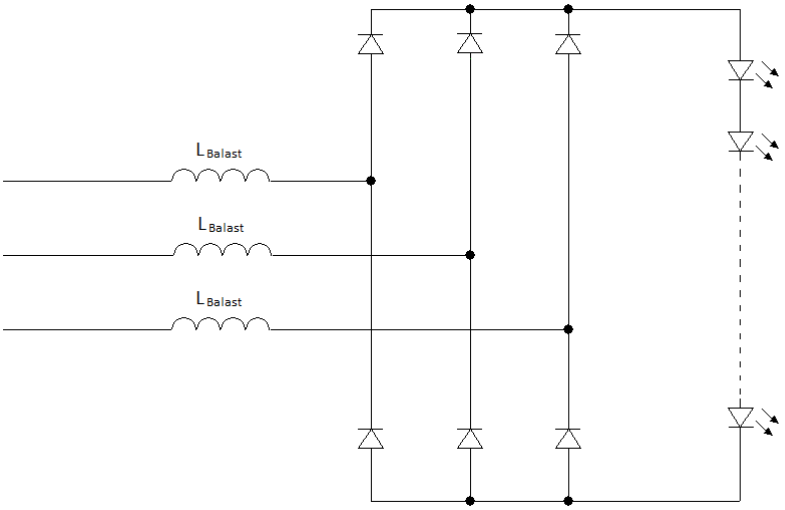

Figure 2.4: B6 three-phase LED driver

2.3 Experiment

The structure of the practical experiment is shown in figure 2.5. The test report is attached in appendix section D. This system has been built up and tested in the laboratory. The used supply voltage source was a regulation transformer with the ability to adjust the supply voltage from 0 - 230V effective with a constant frequency of 50Hz.

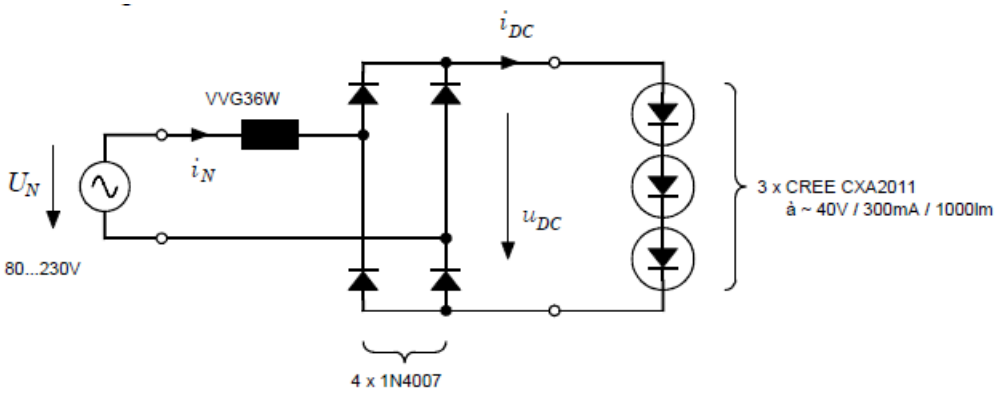

Figure 2.5: Structure experimental test single-phase system

2.3.1 Components

The used inductor for the experiment (see figure 2.6) is taken from a conventional fluorescent lamp. Originally the function of the inductor, also called choke ballast, is to limit the current through the lamp in service. In most lamps the inductor is also used to produce a voltage spike to strike the arc in the lamp when it is switched on. The letters VVG stand for low loss ballast (Verlustarmes Vorschaltgerät). The VVG ballasts were developed in the past to substitute the conventional ballasts for reducing losses. Nowadays, the choke ballasts are replaced by electronic circuits (electronic ballasts).

Figure 2.6: Conventional inductor VVG36

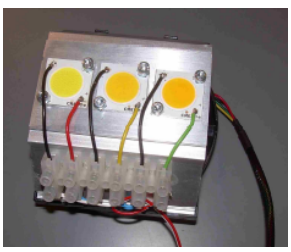

Figure 2.7: Used LEDs 3 x Cree CXA2011

The used LEDs for the experiment are pictured in figure 2.7. It is here dealt with three 40V-LED units from the company Cree. The three units are connected

in series as pictured in figure 2.5. In figure 2.7 the three units are mounted side by side on a cooling element to keep the operating temperature low. The electrical characteristic of one LED unit is pictured in figure 2.8. Observable in the figure is a wide operating span. The operational current lays from 100 - 1000mA. The LED current was in the experiment raised to a maximum of 350mA(AVG.).

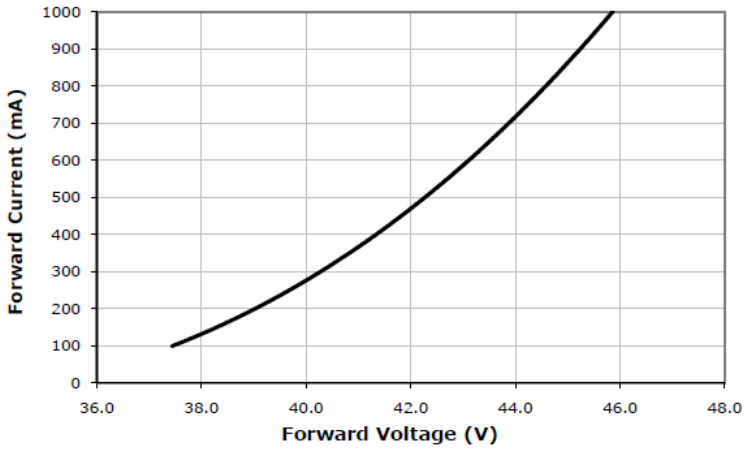

Figure 2.8: Electrical Characteristics CREE CXA2011 [1] (TJ = 85 °C)

2.3.2 Results experiment

The results from the measurements are plotted into figure 2.9. The measurements were read and noticed in 10V steps of the supply voltage. The supply voltage was adjusted in the range from 80 - 230V. I would like emphasize that the left vertical axis in figure 2.9 has the unit Watt and percent at the same time. The taken power from the grid and the taken power from the LEDs refer to the axis in Watt. The values for the efficiency of the inductor $\frac{P_{Led}}{P_{Grid}}$, the total harmonic distortion(THD) and the power factor(PF) are in percent. The values for the grid current and the LED current are normalised in ratio to the values by full load, when the supply voltage is by 230V. The grid current was by 405mA(RMS.) and the LED current by 352mA(AVG.) at 230V. The current values therefore refer to the axis in percent of the full load current. The absorbed power in the LED unit is measured on the basis of mean values in current and voltage drop. The right vertical axis refer to the orange trend which represent the measured light intensity in kilo lux. For the measurement a lux meter of the type PAN LX 1308 was used from the manufacturer pancontrol. The photo detector was mounted 27cm from the LED units.

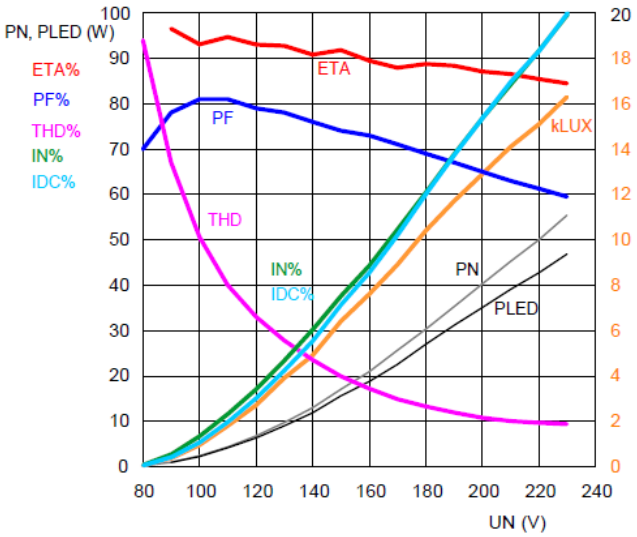

Figure 2.9: Results experiment
PN=Grid power, PLED=LED power, ETA=Efficiency inductor, PF=Power factor(grid)
THD=Total harmonic distortion(Grid current), IN 405[mA](RMS)=100%
IDC 351[mA](avg.)=100%, Klux=light intensity(kilo-Lux)

Figure 2.10 shows interesting oscilloscope wave-shapes when the supply voltage was at 230V. The left picture shows the current taken from the grid(yellow) together with the voltage signal after the inlet of the rectifier bridge(blue). The right picture shows the voltage drop over the LED unit(blue) and the LED current(yellow).

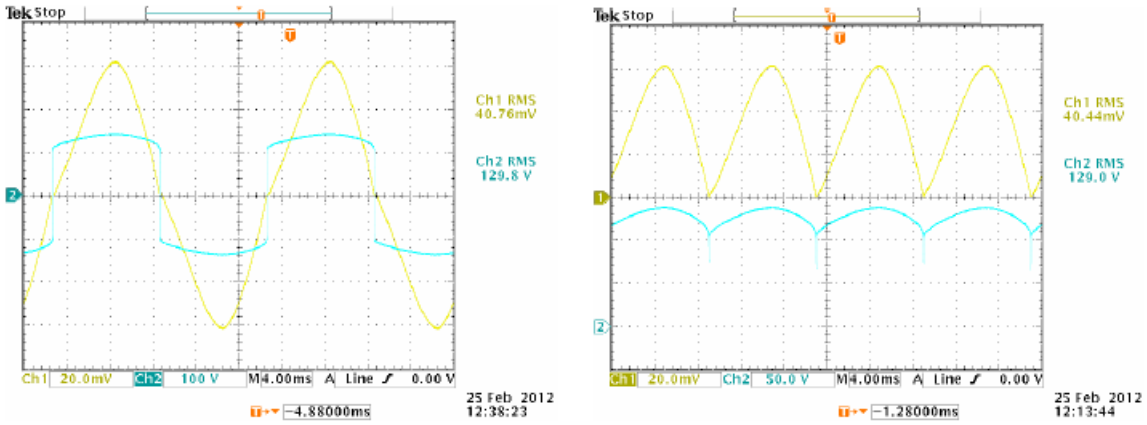

Figure 2.10: $V_{grid} = 230[V]$
left fig:Yellow(Grid current,200[mA]/div), Blue(Bridge voltage,100[V]/div)
right fig:Yellow(i_{DC},200[mA]/div), Blue(u_{DC},50[V]/div)

2.4 Lifetime prediction

Generally, lifetime of technical products is difficult to predict because failures can be caused by other things than the common "wear out" effect. Failures can occur shortly after bringing products into service. Examples of early deficiency are failures in the mounting process or errors in the applied materials. This issue is often graphically expressed in the known bathtub curve.
LEDs experience a decrease in the amount of light they emit over time, this process is known as lumen depreciation. A level of acceptable lumen depreciation must therefore be chosen to define at what point the light level no longer meets the requirements for the application. The answer may differ depending on the application of the product. A 30% reduction of the light intensity has become the standard threshold for illuminating systems as useful life. The 30% reduction is in general terms written as L70 which means the light output has declined to 70%.
Predicting the lifetime of LEDs generally involves many difficulties. One problem with predicting the lifetime of new LEDs lays in the fact that the used technology continues to develop and evolve so quickly, that products would be obsolete by the time they finished life testing [2]. Notably, testing a LED for 50.000 hours takes 5.7 years when it is operated 24/7. Producers commonly use an estimation method to predict the lifetime of their products.
The Illuminating Engineering Society of North America (IESNA) have made a guidance to how LED lifetime (L70) mathematically can be predicted. The guidance LM 80-08 from IESNA describes the testing and measuring part, for the LEDs which need a lifetime prediction. In TM-21-11 from IESNA a method for making lifetime projections on the basis of LM 80-08 data is specified. The testing and measuring part (LM 80-08) requires among other things at least a testing period of 6000 hours for the considered LEDs. With the measured lumen depreciation from the testing period a lifetime prediction by means of TM-21-11 is performable. One among other requirements for the testing part, described in LM 80-08 requires, that the LED current has a ripple below 2%.

In figure 2.11 an example of a lifetime prediction is pictured from the company Philips [3]. The curve shows the light depreciation for a white power LED they call LUXEON Rebel by 85 °C and 350mA.
Nevertheless, two important factors to obtain longer lifetime is to keep the junction temperature low and not to allow higher currents as the manufacturers recommend [2].

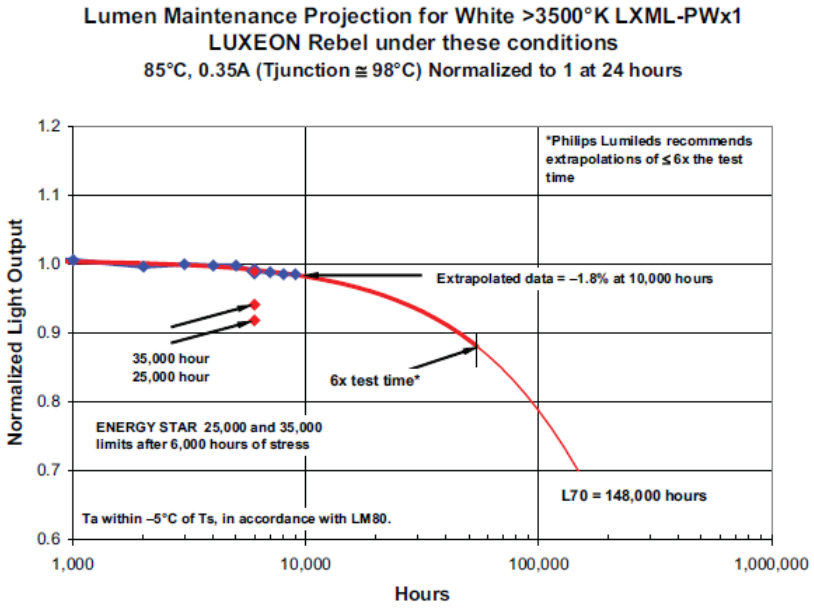

Figure 2.11: Lifetime (L70) white LED from Philips [3]

The curve in figure 2.11 represents the mentioned wear out effect, when lumen deprecation takes place. With a catastrophic failure in a LED, an instant failure occurs. Here an electrical open and an electrical short failure can occur. The open failure cuts of the power supply for the rest of the LEDs in the string and the lamp will remain dark. To counteract this failure a Zener diode is suggested. The idea is to apply a Zener diode with a Zener voltage higher as the LED voltage drop parallel to every LED. This will lead the current past the LED with an open failure. However Philips claim that the chance for a catastrophic failure is extremely low, for their LUXEON Rebel series.

Another component in the represented passive LED device is the inductor. The lifetime of an inductor according to [4, P. 89] is following the Arrhenius equation. This equation is strongly dependend on the operation temperature of the inductor. This means that lifetime increases with lower operating temperature and decreases with higher operating temperature. Actually the lifetime rate doubles by every step the operating temperature decreases by 10 °C or, contrariwise, lifetime is halved when the temperature is increased by 10 °C. The company Tridonic also assumes that magnetic chucks produced by them [5] follow the Arrhenius equation, when it comes to lifetime prediction. Tridonic has for many years produced magnetic chokes for fluorescent lamps.

The vertical axis in figure 2.12 describes lifetime in years if the choke is operated constantly 24/7. Tridonic claims that their chokes have a lifetime expectancy of 100.000 hours if operated by 130 °C, which approximately equates 10 years of non-

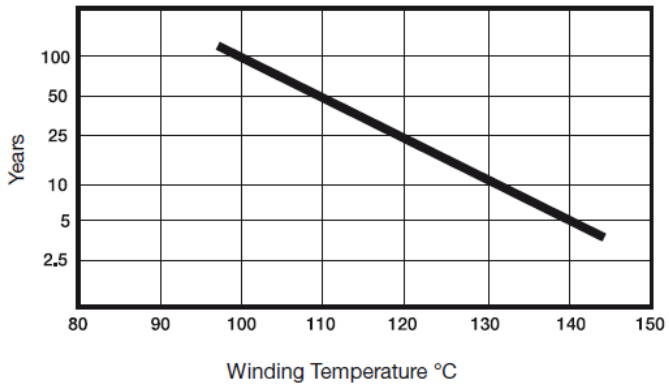

Figure 2.12: Lifetime prediction magnetic chokes from company Tridonic [5]

stop operating.

At last the diodes for the rectifier bridge in the LED driver have to be considered. Here the idea is to pick some oversized diodes for this operation. An example of oversized diodes could be of the type 1N4007, designed for a RMS reverse voltage of 1000 V. This diode meets the demand for both LED drivers represented in section 2.2.

2.5 Modeling led

For the calculations in section 3 and 4 a mathematical model of a LED is necessary. To counteract this problem the approach is taken for a LED available on the market. The chosen LED is a white power LED from the manufacture Lite-On. The LED has, at the nominal operation point, a forward current of 350mA and a voltage drop of 3.8V. The nominal voltage drop over most of the offered white LEDs are around 3.5 V in service. The nominal LED current thereby is offered in a wider span. In section 3.3 it will be shown that the 350mA suits the intention of the circuit quite well. Figure 2.13 shows the I-V characteristic of the LED. The characteristic is being approximated as linear around its working point between 100 and 350mA, see figure 2.14.

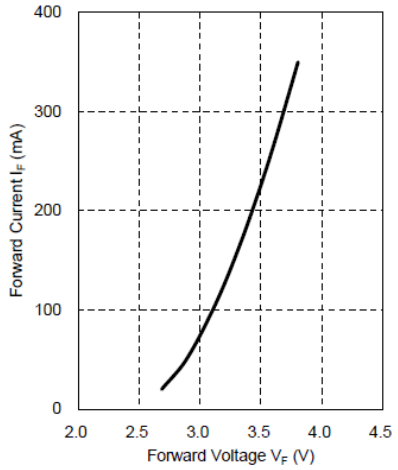

Figure 2.13: LED V/I characerisic [6]

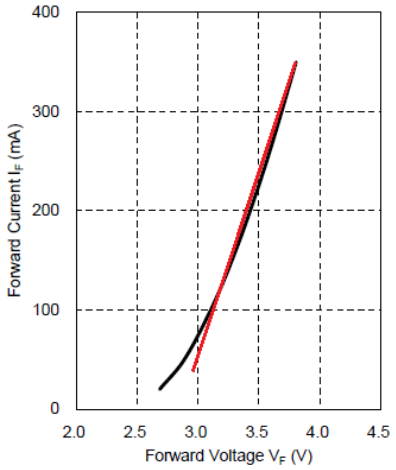

Figure 2.14: linearised led

The resistive part of the LED is approximated by the equation

$$r_{Led} = \frac{\Delta v_{Led}}{\Delta I_{Led}} \tag{2.1}$$

in this case using the LED from Lite-On the resistance will be approximately

$$r_{Led} \approx \frac{3.8 - 3.1[V]}{0.35 - 0.1[A]} \approx 2.8[\Omega] \tag{2.2}$$

According to the data sheet [6] the LED has at nominal service by 350mA a voltage drop of 3.8V. To full fill the linear approach for the LED around its working point following equation must be valid

$$V_{Led}[V] + 0.350[A] \cdot r_{Led}[\Omega] = 3.8[V] \tag{2.3}$$

This results in an equivalent voltage source of 2.82V. The equivalent circuit hereby becomes a series connection of a resistor and a DC voltage source with the above calculated values. According to the data sheet [6] the area between 100 and 350mA will give an almost linear proportional variation in the light intensity from 36 to 100%, see figure 2.16.

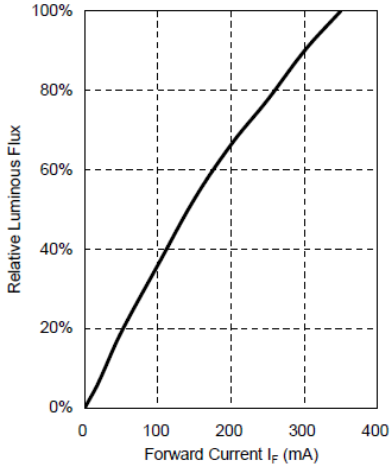

Figure 2.15: Characteristic flux and current [6]

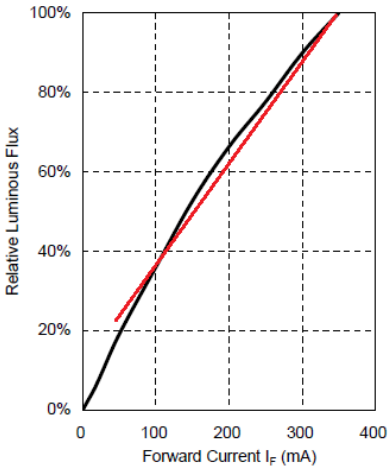

Figure 2.16: linearised flux

Noticeable is that the characteristic of a LED is addicted to the operating temperature. According to the data sheet of the chosen LED above the forward voltage V_F from figure 2.13 change by -2mV/°C in nominal service at 350mA.

3 Single-phase system

3.1 Calculation method ideal circuit

For the calculations, the circuit in figure 2.3 has been changed to the equivalent circuit of figure 3.1. The following equations are therefore only valid for the idealized circuit given in figure 3.1 and do not correspond completely with the real circuit. The ideal approach is carried out with the purpose to give a clear overview of how the circuit acts. Later the real circuit will be simulated with PSPICE and compared with the calculations from this section. In the following equations the value for V_{Grid} is set as effective value of the phase-to-neutral voltage.

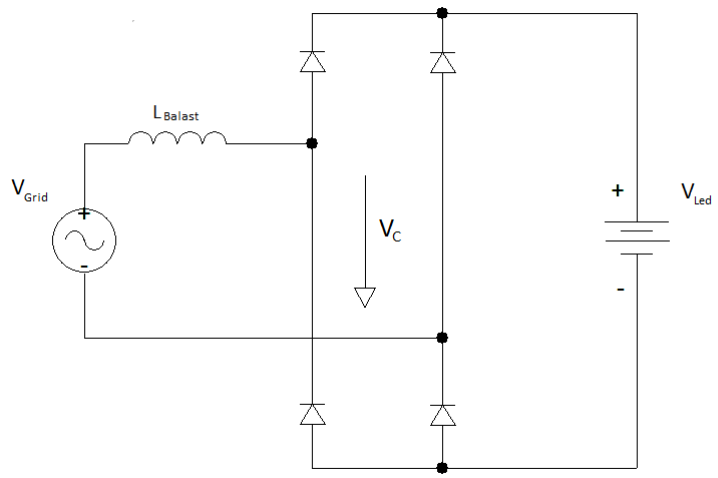

Figure 3.1: B2 ideal equivalent circuit

By only considering the circuit in figure 3.1 the following neglections have been done:

- Neglecting internal impedance of connected power grid V_{Grid}
- Neglecting resistive part from LEDs
- Neglecting voltage drop and resistive part from diodes in B2 bridge
- Neglecting resistive part from inductor
- Assuming the inductance of the inductor is linear
- Assuming the supply voltage V_{Grid} is an ideal sine wave

- Assuming that $V_{Led} < V_{Grid} * \frac{\sqrt{2}}{2}$

If the voltage from the connected power grid and the voltage by the AC inlet of the B2 bridge V_C is observed, it is possible with a Fourier analysis of the V_C signal to calculate characteristic parameters like current, power, phase and power factor. In figure 3.1 the signal V_C becomes a rectangular harmonic switching signal between the values $+V_{Led}$ and $-V_{Led}$ when the ideal circuit is operated under the above mentioned last assumption.

The term $V_{Led} < V_{Grid} * \frac{\sqrt{2}}{2}$, with V_{Grid} as an effective value, is made to keep the Fourier analysis simple. If V_{Led} becomes greater than $V_{Grid} * \frac{\sqrt{2}}{2}$ the V_C signal will no longer be a continues rectangular signal but turn into a discontinuous signal which will deliver a different and more complex Fourier series as the one presented below. The voltage drop V_{Led} is at the beginning being considered as a continuous selectable signal and later the limitation for V_{Led} in approximately 3.5 voltage steps will be passed through.

The Fourier series which suits the periodic rectangle signal in this case can be calculated with the equation

$$V_C(t) = \frac{2}{\pi} \int_0^{\pi} f(t) sin(n \cdot \omega t) dx \tag{3.1}$$

derived from the common Fourier display format. With the consideration that the periodic rectangle signal is an even function which oscillates with a frequency of 50 Hz the display format for the voltage signal V_C with a Fourier series looks as follows

$$V_C(t) = V_{Led} \cdot \sum_{n=1,3,5..}^{\infty} \frac{4}{\pi n} sin(n \cdot 2\pi 50 \cdot t) \tag{3.2}$$

If assumed that the supply voltage is an ideal sine wave, with 50Hz free from harmonic oscillations of order greater than 1, following equation

$$V_{1.L} = V_{Grid} - V_{1.C} \tag{3.3}$$

can be used to calculate the voltage drop on the inductive ballast for the voltage fundamental. Further the vector diagram in figure 3.2 can be created. Mentionable here is that the current $I_{1.grid}$ refers to the effective value of the fundamental harmonic of the current, taken from the grid and not the total flowing current.

In figure 3.2 ϕ_1 represents the angle between the voltage V_{Grid} and the funda-

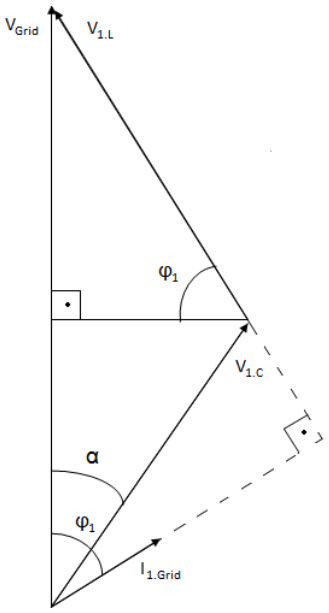

Figure 3.2: Vector diagram single-phase LED driver

mental of the grid current $I_{1.Grid}$. The angle α represents the angle between the V_{Grid} and the rectangle signal generated from the B2 bridge which also will be the angle between V_{Grid} and the $V_{1.C}$ signal. Finally, the fact that the current $I_{1.L}$ is delayed by 90 degrees in relation to the voltage drop $V_{1.L}$ allows to create following equations via the shown geometry in figure 3.2.

$$V_{1.L} = I_{1.Grid} \cdot \omega L_{Balast} \tag{3.4}$$

$$V_{1.C} = \frac{4}{\pi\sqrt{2}} V_{Led} = \frac{\sqrt{8}}{\pi} V_{Led} \tag{3.5}$$

$$V_{1.C} \cdot sin(\alpha) = V_{Grid} - V_{1.L} \cdot sin(\phi_1) \tag{3.6}$$

$$V_{1.C} \cdot sin(\alpha) = V_{1.L} \cdot cos(\phi_1) \tag{3.7}$$

$$\alpha = arccos\left(\frac{V_{Led} \cdot \pi}{\sqrt{8} \cdot \hat{V}_{Grid}}\right) \tag{3.8}$$

The last relation in equation 3.8 is found by observing the voltage signals in figure 3.3. The relation is found following the consideration that the integral of the voltage drop over the inductor must be 0 over a period when the driver works in stationary mode. This fact can be expressed in the following equation

$$\int_{\alpha}^{\alpha+\pi} (\hat{V}_{Grid} \cdot sin(x) - V_{Led})dx = 0 \tag{3.9}$$

which in mathematical graphical terms means that the left shaded area must be equal the right grazed area.

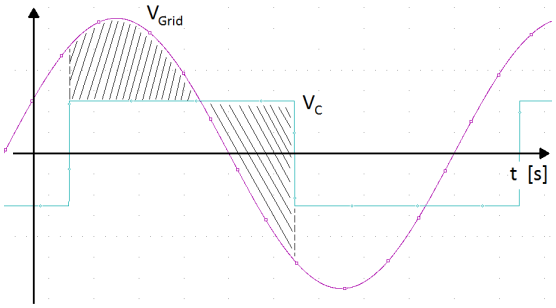

Figure 3.3: Voltage signals single-phase LED driver
$|V_C| = V_{Led}$

With the 5 equations from number 3.4 to number 3.8 it is possible to determine interesting values of the circuit which are essential for studying the performance. The first job is to determine the optimum value for the inductor L_{Balast} and to find out what voltage drop is suitable for the series connection of the LEDs. This is important in order to achieve acceptable values for the current, power consumption,THDi and displacement.

3.2 Function of ideal circuit

The exact derivation of the following results are in detail presented in appendix A. Interesting is that the equation for the power factor PF and the value for the total harmonic distortion THDi is independent from the size of the inductor and only dependent on the chosen V_{Led} and the adjusted voltage V_{Grid}. This issue is shown in figure 3.4. THDi stands for the ratio between the the sum of all harmonic components to the fundamental component in the current flowing from the connected power grid. The approach for the equation is shown below.

$$THDi = \sqrt{\frac{I_{n.UH}^2}{I_1^2}} = \sqrt{\frac{I_2^2 + I_3^2 + I_4^2 ...}{I_1^2}} \tag{3.10}$$

The complete analytical calculation of THDi and PF is in detail represented in appendix A section A.4 and A.5.

$$THDi = \sqrt{\frac{V_{Led}^2(\pi^4 - 96)}{12 \cdot \pi^2 \cdot V_{Grid}^2 + V_{Led}^2(96 - 24 \cdot \pi^2)}} \tag{3.11}$$

$$PF = \frac{V_{Led}}{V_{Grid}} \sqrt{\frac{96 \cdot V_{Grid}^2 - V_{Led}^2 \cdot 12 \cdot \pi^2}{V_{Grid}^2 \cdot 12 \cdot \pi^2 + V_{Led}^2 \cdot \pi^2(\pi^2 - 24)}} \tag{3.12}$$

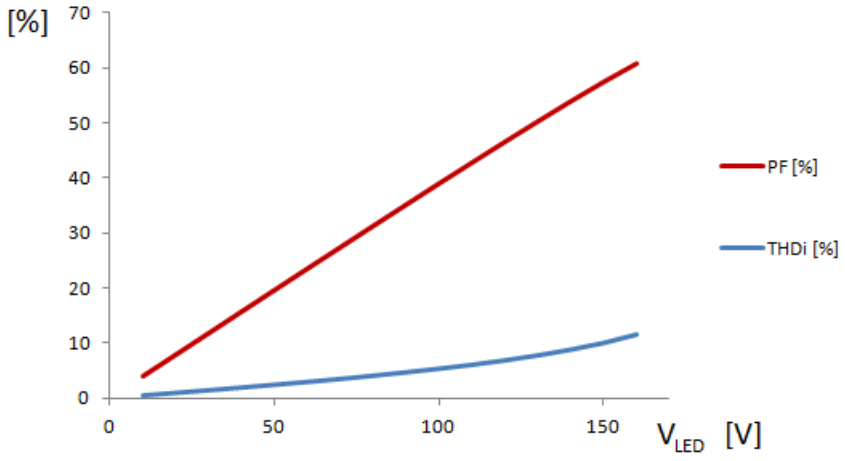

Figure 3.4: Calculation result , $V_{Grid} = 230$[V]
PF and THDi as a function of V_{Led}

Figure 3.4 shows the results of PF and THDi when the voltage from the supply grid is kept at 230V, which is the value where the circuit is supposed to operate normally. On the basis of figure 3.4 the size of V_{Led} can be chosen, when certain values of PF and THDi are supposed to be achieved.

Further the power consumption as a function of the inductor size can tell about the required inductor size for a chosen operating area. The derivation of the power consumption in appendix A.3 equation number A.3.2 is again listed up here:

$$P_{Grid} = \frac{V_{Led}}{\omega L}\sqrt{\frac{8}{\pi^2}\cdot V_{Grid}^2 - V_{Led}^2} \tag{3.13}$$

The calculated power consumption is the one delivered by the AC inlet of the ideal circuit in figure 3.1. This power consumption matches the dissipated power from the LEDs in the ideal circuit. The real circuit will differ from that due to power losses intern in the inductor and of the diodes from the B2 bridge.

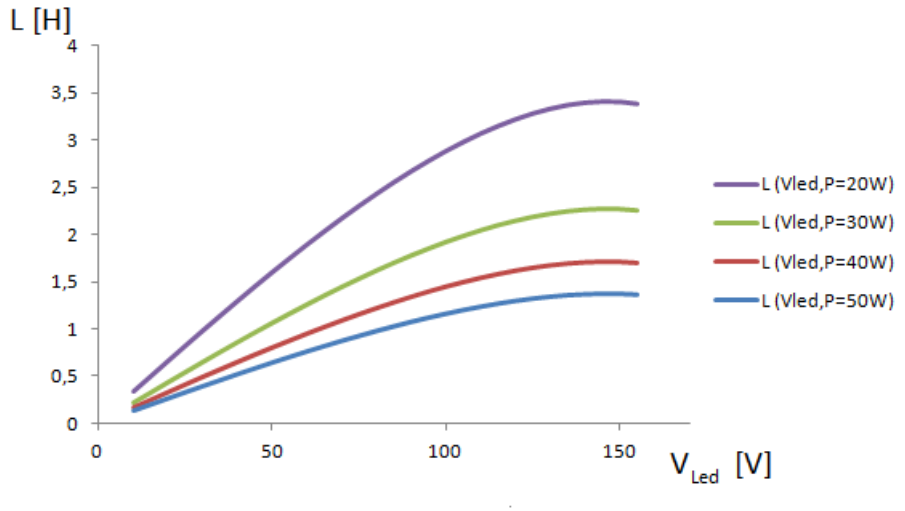

Figure 3.5: Calculation result , V_{Grid}= 230[V]
Inductor size as a function of V_{Led} and power consumption

In figure 3.5 the necessary size of the inductor can be read from the desired V_{Led} and power consumption derived from equation 3.13. The same approach can be followed for the LED current. Considering the average current through the LEDs makes it simpler to pick an suitable LED for the circuit.

Setting equation 3.15 equal $V_{Led} \cdot I_{Led.avg}$, which suits the ideal circuit, the following equation can be made by reshaping

$$L = \frac{1}{\omega \cdot I_{Led.avg}}\sqrt{\frac{8}{\pi^2}\cdot V_{Grid}^2 - V_{Led}^2} \tag{3.14}$$

The plot of equation 3.14 is illustrated in figure 3.6. When looking into figure 3.5 and 3.6 it becomes clear that the inductance value of the required inductor increases when a small power consumption or LED current is desired.

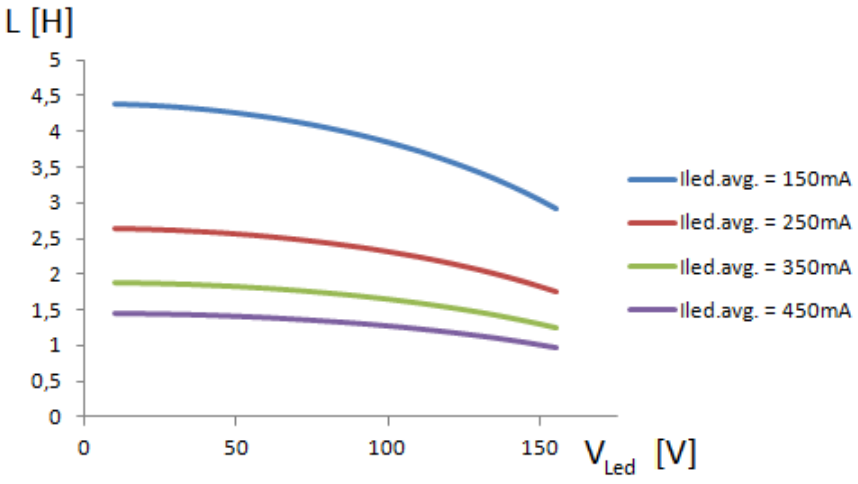

Figure 3.6: Calculation result, $V_{Grid} = 230[V]$
Inductor size as a function of $I_{Led.avg}$ and V_{Led}

3.3 Example ideal circuit

With the purpose to give an example of an plausible circuit the voltage signal V_{Led} is chosen to be around 125V. It is obvious that a balance between PF and THDi must be chosen with help from figure 3.4. A larger PF is of course preferable, but due to the fact that THDi increase together with PF a favoured operating point must be chosen. The 125V will result in an PF around 48.3% and a THDi of 7.36% when the supply voltage is 230V. Further it is chosen that the LED lamp should perform approximately 45 watt. This results in an average LED current of

$$I_{Led.avg} = \frac{P_{Grid}}{V_{Led}} = \frac{45}{125} = 360[mA]$$

The white power LED from section 2.5 is chosen as light source. The voltage drop of 3.8V results in

$$\frac{125}{3.8} \approx 33$$

LEDs in series. 33 LEDs in series gives an V_{Led} of 125.4V. To achieve an average current of 350mA by 33 LEDs in series an inductor of approximately 1.5H is necessary. Due to the fact that the above made Fourier series in equation 3.5 only is valid under the condition that $V_{Led} < V_{Grid} * \frac{\sqrt{2}}{2}$ the plot in figure 3.7 is limited for the area:

$$125.4 \cdot \sqrt{2} \;<\; V_{Grid} \;<\; 250 \quad [V]$$

In figure 3.7 the rated power is in the region of 26.3W to 49.7W under the above mentioned area of V_{Grid}. This equates an dimming effect of 53% in the respective area for the ideal circuit shown in figure 3.1.

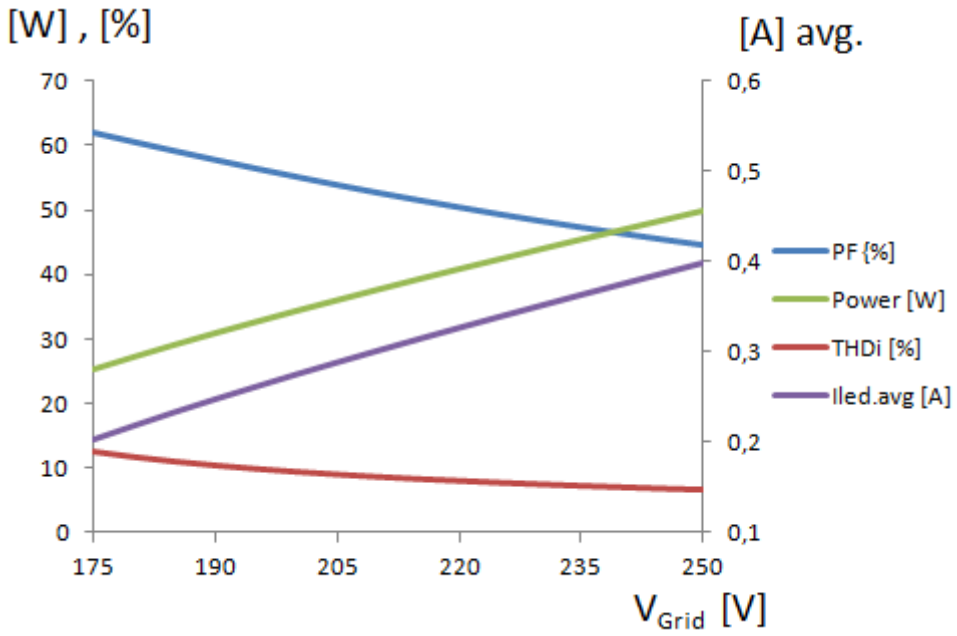

Figure 3.7: Results of calculation, L = 1.5[H], V_{Led} = 125.4[V]
PF, THDi, P and $I_{Led.avg}$ as a function of V_{Grid}

3.4 Simulation B2 circuit

Next the model of the real LED driver is analyzed with the simulation program Pspice. It is the equivalent circuit to the real LED driver with the chosen 33 white LEDs connected in series which is analyzed further. Pspice is used to give a picture of how different parameters like THDi, PF, power and current behave when the supply voltage from the grid is going below the term $V_{Grid} < V_{Led} \cdot \sqrt{2}$ and generates a discontinuous grid current. In addition the resistive part of the circuit also is applied to the simulated circuit. In figure 3.8 the structure of the real circuit is illustrated.

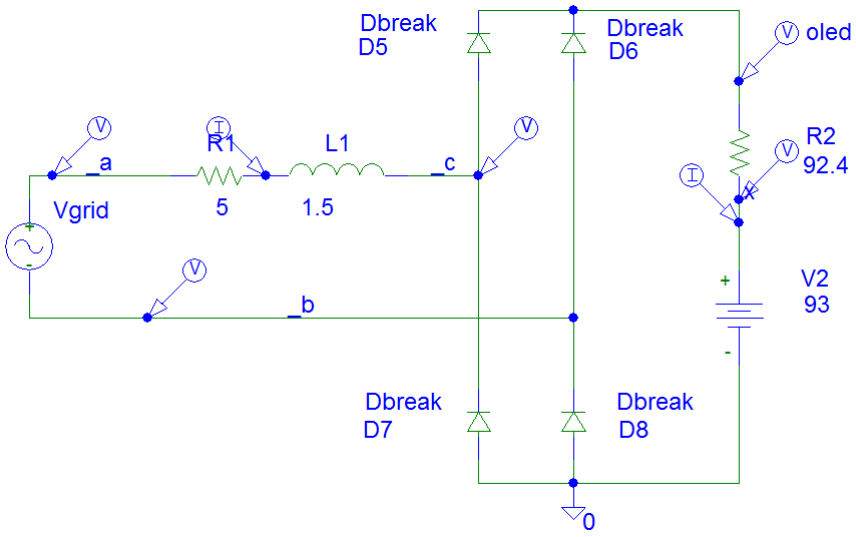

Figure 3.8: Pspice real equivalent circuit for simulation
$R_L = 5[\Omega], L = 1.5[H], R_{Led} = 92.4[\Omega], V_{Led} = 93[V]$

The resistive part R_{Led} represents the sum of the resistance from each LED. The size of R_{Led} becomes

$$R_{Led} = 2.8[\Omega] \cdot 33 = 92.4[\Omega] \tag{3.15}$$

where the 2.8Ω represents the resistance of one white LED derived in equation 2.2. The "threshold" voltage of 2.82V for each LED was derived in section 2.5. The size of the equivalent direct voltage source for the simulation becomes:

$$V_{Led} = 2.82 \cdot 33 \approx 93[V] \tag{3.16}$$

It is obvious that the characteristic of the LED is not perfectly linear, especially

when the voltage drop decreases down near the "threshold" voltage. When looking into figure 2.13 the chosen values picture the behaviour of the circuit quite accurate as long as the LED current stays above 80 mA. The resistive part of the inductor R_{Balast} is set to 5Ω. Even though the yoke and the windings of the inductor is not designed here, the size of the resistive part is set to 5Ω.

The simulation has been realized with the transient analysis function in Pspice. With this function the circuit with the shown parameters in figure 3.8 has been simulated with a variable supply voltage source V_{Grid}. 18 separate simulations have been executed where V_{Grid} has been changed in 10V steps by every simulation from 70V to 240V. At the end of every simulation, characteristic values were noticed and put into the table in figure 3.10. The transient function in Pspice offers among other things a Fourier analysis of a chosen signal. In figure C.1 from appendix section C the setup of the parameters for the transient analysis can be seen. The chosen signal for the Fourier analysis is the I(R1) signal which equals the grid current. The center frequency is set to 50Hz and the number of harmonics is set to 100. According to DIN 40110 a multiple of 40 to 50 is sufficient when calculating THD values. The setting of 100 should therefore deliver a quite accurate THD value.
Noticeable is that the transient function makes the Fourier analysis of the last full period of the chosen signal. The final time for the simulation is adjusted to 800mS which guarantees the major accomplishment of the transient oscillations. The result of the Fourier analysis can be found in an output file. This file can be accessed via the analysis menu. A part of the output file is pictured in figure C.2 appendix section C. The red marked values in figure C.2 show respectively the first Fourier component and the phase angle between the first component and the supply voltage. Further the calculated THD value from the grid current is shown at the bottom in figure C.2. The rest of the required values for the examination of the circuit have been taken from the probe-file which appears when the simulation is carried out. In figure 3.10 the table with all characteristic values from the simulation is arranged.

The trend of the most interesting values from the simulation, taken from the table, is pictured in figure 3.9. The values in the plot show the most important parameters of the circuit behave under service, and when the grid voltage is adjusted for dimming.

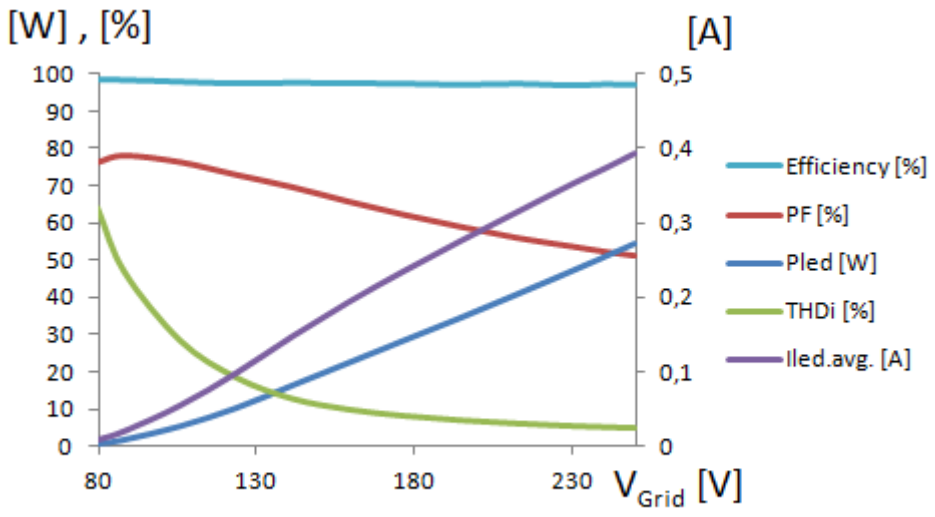

Figure 3.9: Result simulation real equivalent circuit values from figure 3.10

Below in figure 3.10 the values from the simulation are listed up. The supply voltage in the left column was adjusted to the respective value and after that the values in the row to the right were noticed from Pspice.

Vgrid [V]	Igrid.rms [mA]	Pgrid [W]	PF [%]	I1.grid [mA]	φ1 [DEG]	THDi [%]	η [%]	Vled.avg [V]	Iled.avg [mA]	Vled.rms [V]	Iled.rms [mA]	Pled [W]
240	416,8	52,0345302	52,0179	588	58,57	5,26	97,243	127,35	371,5	128,55	417	50,6
230	394	48,247979	53,2421	555,8	57,74	5,57	97,351	125,4	351	126,5	394	46,97
220	370,5	44,6241898	54,7469	522,9	56,73	5,91	97,257	123,5	329,8	124,45	370,5	43,4
210	347	40,9546799	56,2024	489,8	55,73	6,31	97,181	121,5	308,5	122,4	347	39,8
200	323	37,337422	57,7979	456,1	54,63	6,75	97,221	119,5	287	120,3	323	36,3
190	299	33,7476662	59,4044	421,7	53,44	7,33	97,488	117,46	265	118,17	299	32,9
180	274	30,2594224	61,3532	386,5	52,04	7,96	97,325	115,4	242	116	274	29,45
170	248,7	26,821037	63,4382	351	50,53	8,76	97,312	113,25	219	113,75	248,7	26,1
160	222,5	23,3235356	65,5155	313,6	48,9	9,88	97,327	111	195	111,45	222,5	22,7
150	195,3	19,847912	67,7519	275	47,12	11,2	97,491	108,7	170	109,7	195,4	19,35
140	164,5	16,1542221	70,1443	231,3	45,13	13,33	96,879	106,05	141,4	106,35	164,6	15,65
130	136,6	12,7230693	71,647	191	43,56	16,13	97,461	103,63	115	103,85	136,6	12,4
120	107,7	9,50869754	73,574	149,6	41,49	20,15	97,805	101,17	88,4	101,33	107,7	9,3
110	80,3	6,66187882	75,4203	110,1	38,93	25,69	98,02	98,9	63,7	99	80,3	6,53
100	54,7	4,23525566	77,427	73,7	35,64	33,25	97,751	96,85	41,7	96,9	54,8	4,14
90	32,1	2,2581189	78,1626	41,54	31,33	44,43	98,312	95,1	22,8	95,13	32,1	2,22
80	13,4	0,81840189	76,3435	15,98	25,13	63,61	107,53	93,78	8,46	93,79	13,4	0,88

Figure 3.10: Pspice results from simulation single phase LED driver figure 3.8
$P_{Grid} = V_{Grid} \cdot I_{1.Grid} \cdot cos(\phi 1)/\sqrt{2}$, $PF = \frac{P_{Grid} * 100}{V_{Grid} \cdot I_{Grid.rms}}$, $\eta = \frac{P_{Led} \cdot 100}{P_{Grid}}$

Figure 3.11 show the trace of the grid current when the supply voltage is adjusted to 230V. The lower diagram picture the frequency spectrum of the grid current. Observable is that the spectrum consist of the uneven row starting with the fundamental frequency of 50Hz and than afterwards 150, 250, 350...
Visible is also that the spectrum decays very fast, the content of the ninth harmonic wave(450Hz) is not recognizable in this diagram. The blue trace in the upper diagram shows the trace of the voltage signal at the AC inlet of the B2 bridge (see figure 3.8). Due to the fact that the resistive part has been added to the circuit, the voltage signal is no longer a perfect switching rectangle signal but has become a wave form showing some "ohmic" behaviour.

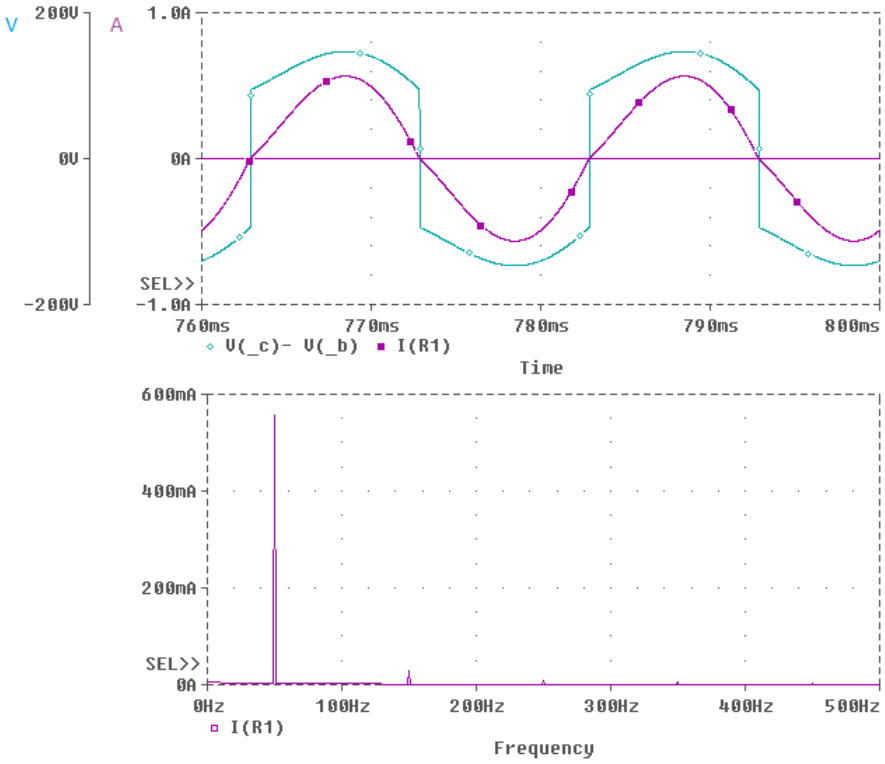

Figure 3.11: Result simulation of figure 3.8 , $V_{Grid} = 230[V]$
Upper diagram: Red(grid current) , Blue(Voltage signal AC inlet B2 bridge)
Bottom diagram: fft of grid current

In figure 3.12 the trace of the LED current is shown in the upper diagram. Visible is that the trace "oscillates" between 0 and approximately 570mA with a frequency of 100Hz. This also means that the LED current may generate stroboscopic oscillations with a frequency of 100 Hz. The average value of the LED current is by 351mA, this is shown with the blue trace.

The bottom diagram shows the trace of the total voltage drop over the series connection of the equivalent resistor and voltage source(V2 and R2) in figure 3.8.

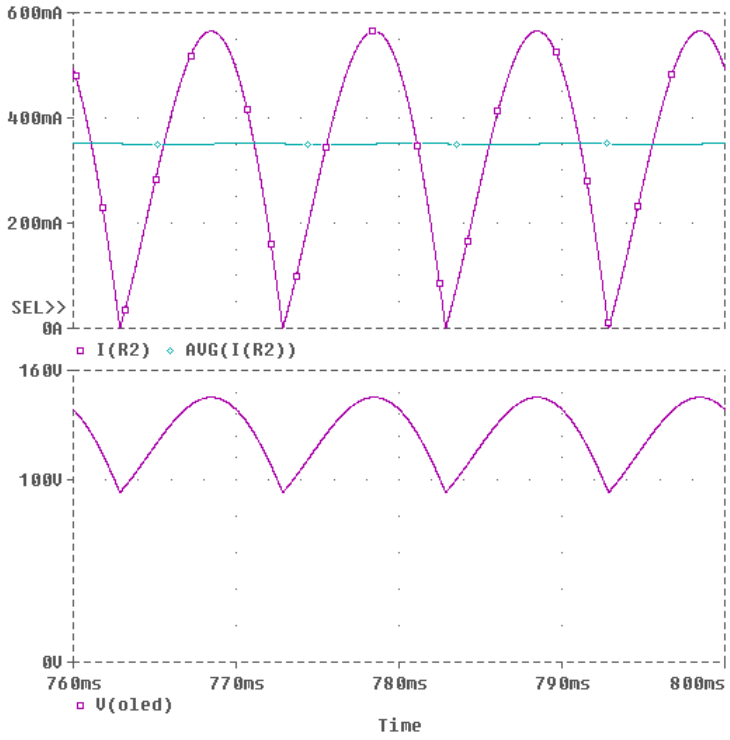

Figure 3.12: Result simulation of figure 3.8 , $V_{Grid} = 230[V]$
Upper diagram: Red(trace LED current) , Blue(AVG. LED current)
Bottom diagram: Voltage drop LEDs

Below in figure 3.13 the trace of the grid current and the voltage signal at the AC inlet of the B2 bridge is shown, when the supply voltage was adjusted to 100V. It can be observed that the grid current (upper diagram, red trace) is zero for approximately a quarter of the period. This issue was implied in section 3.1 together with the calculations. The calculations are only valid for a continuous grid current. This is also the reason why V_{Grid} in figure 3.7 is limited in the area from 175 - 250V. Further the spectrum of the grid current no longer decay as fast as when the supply voltage was by 230V. The content of the third harmonic(150Hz) oscillation have according to figure 3.13 increased significant(bottom diagram).

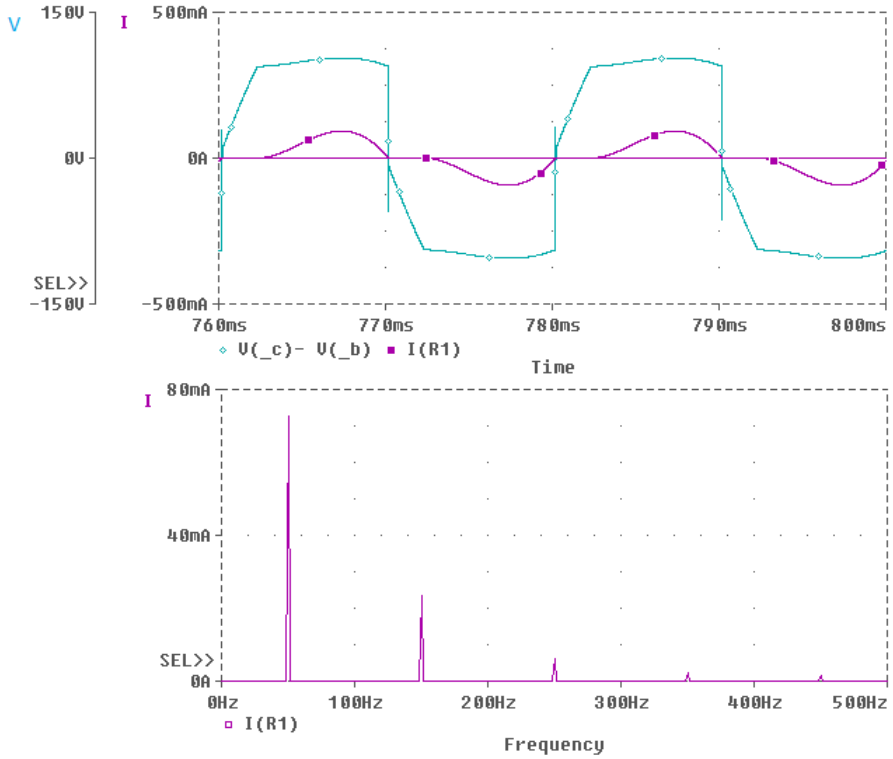

Figure 3.13: Result simulation of figure 3.8 , $V_{Grid} = 100[V]$
Upper diagram: Red(grid current) , Blue(Voltage signal AC inlet B2 bridge)
Bottom diagram: fft of grid current

In figure 3.14 the trace of the LED current is shown. The average value of the current results to 41.7mA.

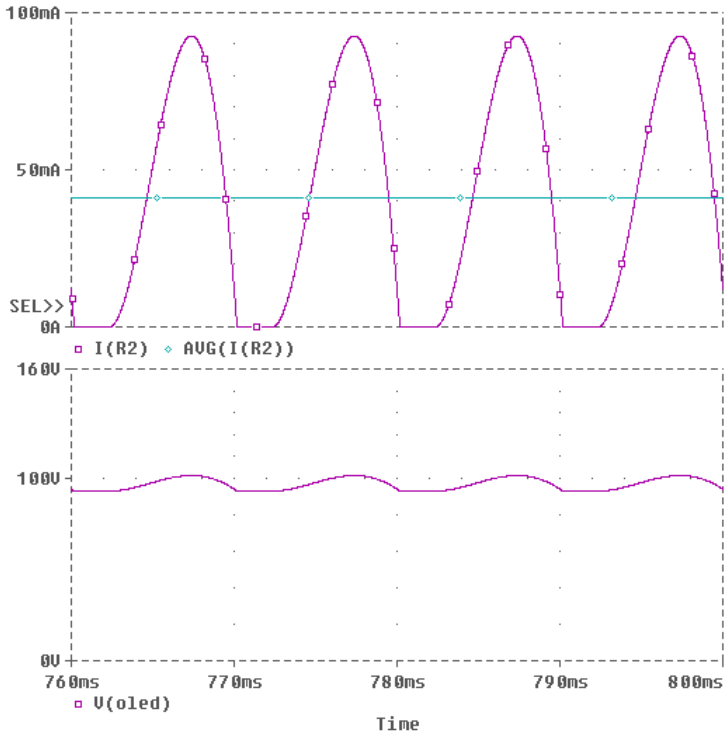

Figure 3.14: Result simulation of figure 3.8 , $V_{Grid} = 100[V]$
Upper diagram: Red(trace LED current) , Blue(AVG. LED current)
Bottom diagram: Voltage drop LEDs

3.5 Discussion of results - calculation and simulation

The theoretical approach of the ideal circuit with the calculations describe the behaviour of the single phase LED driver quite well. The parameters of the simulated circuit with the added resistive part does not differ much from calculated circuit without the resistive part(compare figure 3.7 and 3.9). Considering the THDi values the simulated circuit shows a slightly lower value as the calculated ideal circuit(ideal:7.34%, simulated:5.6% by 230V). This is a result of the added series resistance R_{Led}. Imagine if the modelled LED only would consist of a resistance and no voltage source at all, the value for THDi would be zero. The simulated circuit shows a slightly higher power factor as the ideal circuit(ideal:50%, simulated:53.2% by 230V). This again is a result of the added resistances in the simulated circuit.

3.6 Discussion of results - simulation and experiment

The values from the experiment does differ from the simulated and the calculated values, although the basic characteristic behaviour is in agreement. Important keeping in mind, before the results are compared, is that the experiment was executed with other LEDs as the one used in the simulation. Further a detailed documentation of the used inductor(VVG36) is not existent. In the experiment three LED modules of the type CREE CXA2011 was connected in series. The three modules can be modelled the same way as the LEDs used for the simulation was, if figure 2.8 is considered. This results in a resistance of approximately 29Ω in a series connection with a DC voltage source of 114V. These results occur when each LED module is linearised in the area from 38 to 45V(see figure 2.8). The equivalent resistance and voltage source used for the simulation were 92.4Ω and 93V on the basis of using the LEDs from section 2.5. The simulated LEDs contain a larger resistive part as the LEDs used in the experiment. This fact is observable when the traces of the voltage signals before the bridge is compared with each other(compare figure 2.10 and 3.11). The value for THDi will increase near the theoretical calculated values from the ideal circuit if the resistive part of the LEDs is omitted. This is of course under the assumption that the inductor works linear and the voltage drop over the B2-bridge is neglected. The THDi value in the experiment was by approximately 10% at a supply voltage of 230V. If the LED resistance in the experiment is neglected the voltage signal before the B2-bridge would oscillate between +114V and -114V. This results in a THDi according to the calculations of 6.4% when the supply voltage is by 230V. The difference from the measured 10% and the theoretical 6.4%

must be lead back to the non linear working inductor.
Further the power factor in the experiment was by 59.5%, in the simulation by 53.2% and according to the calculations 48.3% by a supply voltage of 230V. This must be the affect of the higher resistive part in the experiment, which also is observable in the higher ratio of power loss at the experiment(see appendix section D).

4 Three-phase system

4.1 Calculation method B6 circuit

The procedure of how the three-phase circuit is calculated is similar to how the single-phase circuit in section 3.1 is calculated. The following description is therefore kept compact but will point out where the calculation of the three-phase circuit differs from the calculations in section 3.1. The deviation of all the equations below is in detail presented in appendix section B. In the equations presented below the value for the supply voltage V_{Grid} has to be set as the effective value of the phase-to-neutral voltage, which is a factor $\sqrt{3}$ smaller than the phase-to-phase voltage. The structure of the ideal equivalent circuit for the three-phase LED driver, where the calculation is approached, is pictured in figure 4.1.

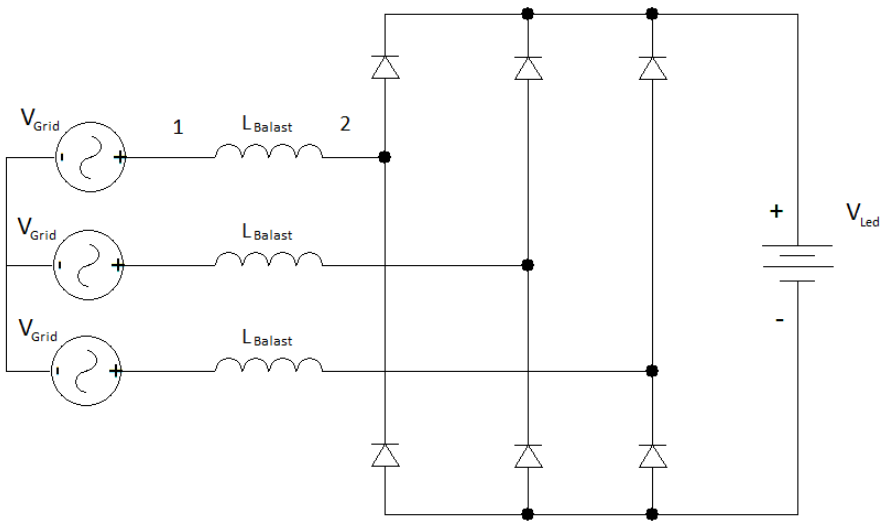

Figure 4.1: B6 ideal equivalent circuit

In order to keep the calculations simple following neglections must be taken into account:

- Neglecting internal impedance of connected power grid V_{Grid}
- Neglecting resistive part of LEDs
- Neglecting voltage drop and resistive part of diodes in B2-bridge
- Neglecting resistive part of inductor

- Assuming the inductance of the inductor is linear
- Assuming the supply voltage V_{Grid} is an ideal sine wave
- Assuming the three-phase supply voltages are symmetric in amplitude and phase
- Assuming that $V_{Led} < V_{Grid} \cdot \sqrt{3}$

The last assumption must be meet due to the fact that the voltage signal presented in figure 4.2 will differ from the shown shape if that term not is considered. Below the basic equations for the calculations are represented. They have been derived similar to how the equations 3.4 - 3.8 in section 3.1 have been derived. Equation 4.3 and 4.4 comes from a identical vector diagram in figure 3.2 where V_{Grid} here, refers to the phase-to-neutral voltage in the three-phase system.

$$V_{1.L} = I_{1.Grid} \cdot \omega L_{Balast} \tag{4.1}$$

$$V_{1.C} = \frac{\sqrt{2}}{\pi} V_{Led} \tag{4.2}$$

$$V_{1.C} \cdot cos(\alpha) = V_{Grid} - V_{1.L} \cdot sin(\phi_1) \tag{4.3}$$

$$V_{1.C} \cdot sin(\alpha) = V_{1.L} \cdot cos(\phi_1) \tag{4.4}$$

$$\alpha = arccos\left(\frac{V_{Led} \cdot \pi \cdot \sqrt{2}}{9 \cdot V_{Grid}}\right) \tag{4.5}$$

Again the mathematical approach is done by observing the voltage signal before and after the inductor similar to the procedure in section 3.1. Significant for this circuit is that the voltage signal in figure 4.1 at point 2, looks like the signal in figure 4.2. Mentionable is that if the circuit is operated beyond the last assumption above, the voltage signal does no longer look like the signal in figure 4.2. In other words the following equations are only valid if the sum of the voltage across the LEDs stay below the effective phase-to-phase value of the supply voltage from the grid.

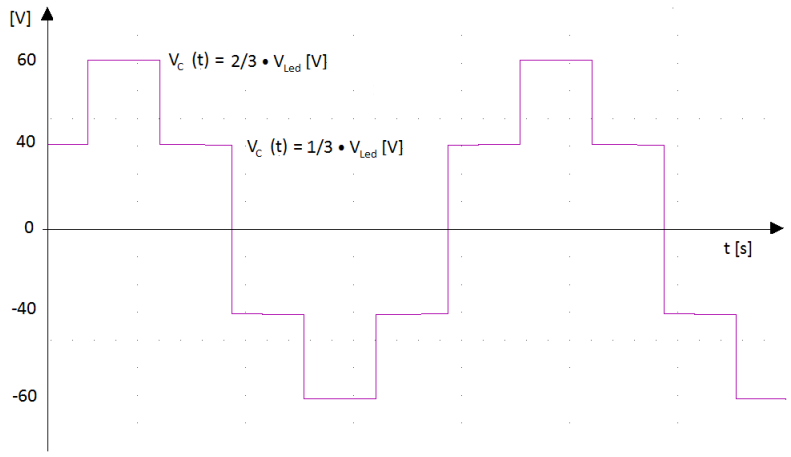

Figure 4.2: Voltage signal three-phase LED driver, $V_{Led} = 90[V]$

Equation 4.2 represents the effective value of the fundamental frequency by 50Hz from this signal. This equation can be derived from the following approach where V_C refers to the signal at point 2 in figure 4.1. The approach for the signal with a Fourier series can be expressed by the following equation:

$$V_C(t) = \frac{2}{\pi}\int_0^{\frac{\pi}{3}} f(t)sin(n\cdot\omega t)dx + \frac{2}{\pi}\int_{\frac{\pi}{3}}^{\frac{2\pi}{3}} f(t)sin(n\cdot\omega t)dx + \frac{2}{\pi}\int_{\frac{2\pi}{3}}^{\pi} f(t)sin(n\cdot\omega t)dx \tag{4.6}$$

This equation delivers the following Fourier series for the signal

$$\hat{V}_{n.C} = \sum_{n=1}^{\infty} \frac{2\cdot V_{Led}}{3\pi\cdot n}\left[1 + cos\left(\frac{\pi\cdot n}{3}\right) - cos(\pi\cdot n) - cos\left(\frac{2\pi\cdot n}{3}\right)\right] \tag{4.7}$$

and equals the expression in equation 4.8. Remarkable is, that only harmonics of order 1, 5, 7, 11.. exist.

$$\hat{V}_{n.C} = \sum_{n=1,5,7,11,13...}^{\infty} \frac{2\cdot V_{Led}}{\pi\cdot n} \tag{4.8}$$

The effective value of the first harmonic oscillation from the voltage signal in figure 4.2 thereby becomes equal the following expression which matches equation 4.2 above.

$$V_{1.C} = \frac{V_{Led}\sqrt{2}}{\pi}$$

Equation 4.5 comes from the integral relation similar to the approach in section 3.2 in equation 3.9.

4.2 Function for ideal circuit

Like for the single-phase LED driver the functions of THDi and PF are for the three-phase system independent to the size of the chosen inductor. The exact derivation of the two functions is represented in appendix section B.4 and B.5. The functions becomes:

$$THDi = V_{Led}\sqrt{\frac{2\cdot\kappa}{V_{Led}^2\left(2-\frac{4\pi^2}{9}\right)+V_{Grid}^2\cdot\pi^2}}; \qquad \kappa = 215.114 * 10^{-5} \tag{4.9}$$

$$PF = \frac{V_{Led}}{V_{Grid}}\sqrt{\frac{V_{Grid}^2\cdot 162 - V_{Led}^2\cdot 4\cdot\pi^2}{V_{Led}^2(162[1+\kappa]-36\cdot\pi^2)+V_{Grid}^2\cdot 81\cdot\pi^2}}; \qquad \kappa = 215.114 * 10^{-5} \tag{4.10}$$

The value κ is generated when the sum of the Fourier series is calculated, the deviation is shown in appendix section B.4. The results for THDi and PF are pictured in figure 4.3.

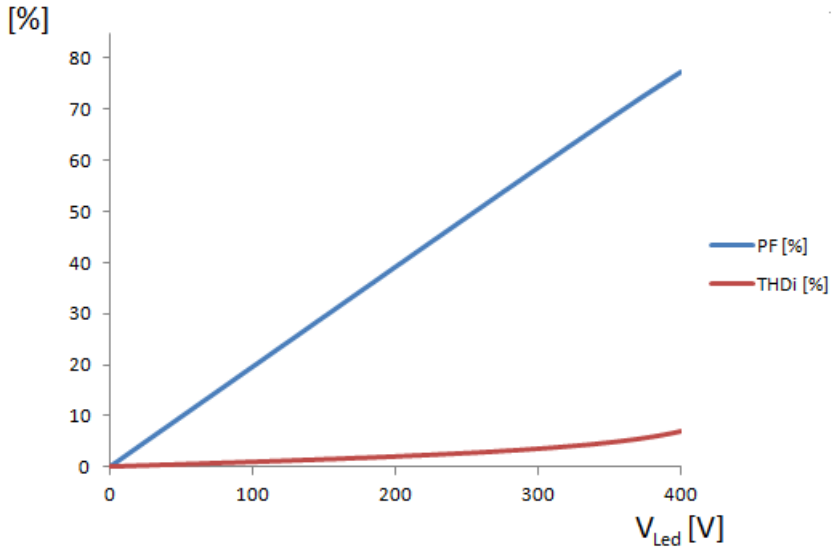

Figure 4.3: Result calculation, $V_{Grid} = 230V$(phase-to-neutral)
PF and THDi as a function of V_{Led}

The above pictured functions are valid for the ideal circuit, when the effective value of the supply voltage is constant at its nominal (400V, effective, phase-to-phase). Next the size of the inductor as a function of V_{Led} and power consumption is expressed. The exact deviation of the power consumption is shown in appendix section B.3.

$$L_{Balast} = \frac{V_{Led}}{\omega P_{Grid}} \sqrt{V_{Grid}^2 \cdot \frac{18}{\pi^2} - V_{Led}^2 \cdot \frac{4}{9}} \tag{4.11}$$

Figure 4.4 displays equation 4.11. This function shows the necessary inductance values of the ballast choke under the favoured power consumption from the ideal unit. The shown relation between power consumption and inductor size is given under the condition that the supply voltage is fix, at its nominal value of 230V phase-to-neutral.

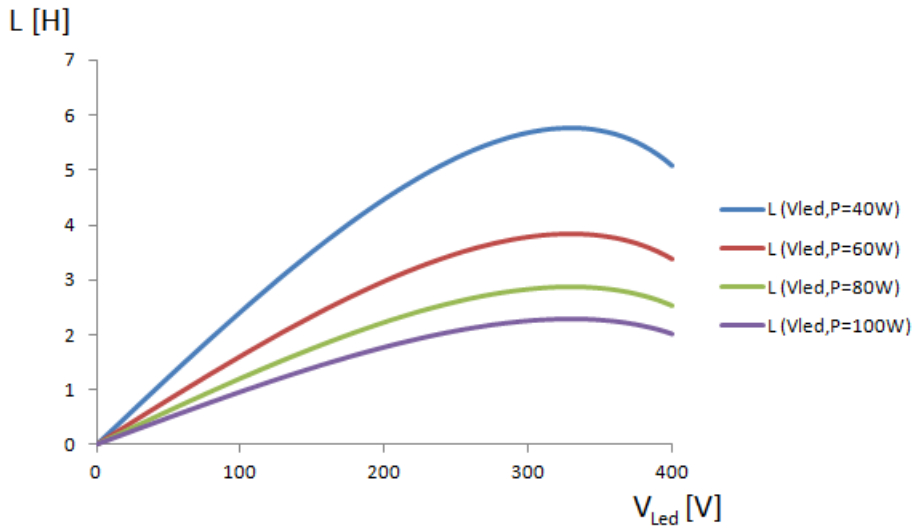

Figure 4.4: Result calculation, $V_{Grid} = 230V$(phase-to-neutral) inductor size as a function of V_{Led} and power consumption

Further by setting the equation for the power consumption equal $V_{Led} \cdot I_{Led.avg}$ the following equation for the average LED current can be expressed.

$$L_{Balast} = \frac{1}{\omega \cdot I_{Led.avg.}} \sqrt{V_{Grid}^2 \cdot \frac{18}{\pi^2} - V_{Led}^2 \cdot \frac{4}{9}} \tag{4.12}$$

Figure 4.5 below represents equation 4.12. The function displays the inductor size as a function of the chosen V_{Led} and the average value of I_{Led}. These functions are again plotted under the condition that the supply voltage is at its nominal value of 230V phase-to-neutral.

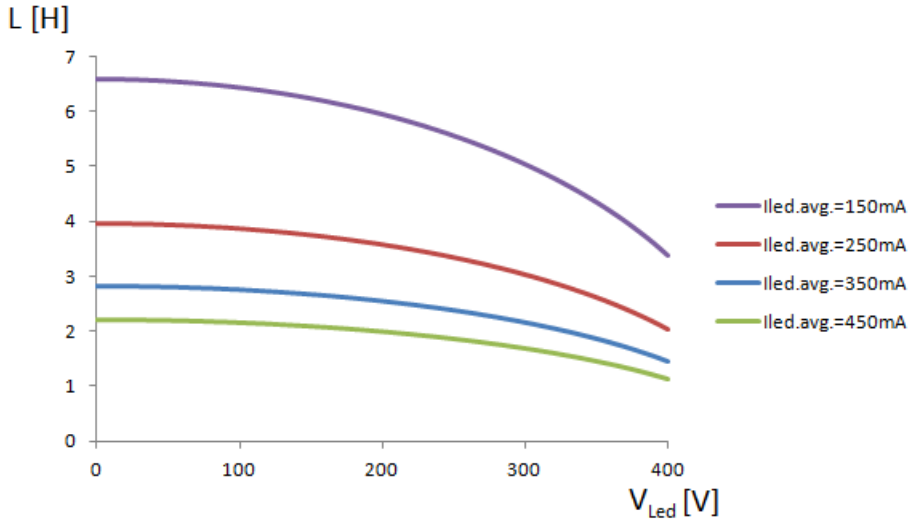

Figure 4.5: Calculation result, $V_{Grid} = 230[V]$(phase-to-neutral) inductor size as a function of V_{Led} and $I_{Led.avg}$

4.3 Example of ideal circuit

To give an example of a circuit the modelled LED from section 2.5 again is used to show the results. Here the voltage drop over the series connection of the LEDs (V_{Led}) is chosen to be 285V. This results in an THDi value of only 3.26% and a power factor of 55.62% when the supply voltage V_{Grid} is 230V (phase-to-neutral). A V_{Led} of 285V results in

$$\frac{285[V]}{3.8[V]} = 75 \ \ LEDs$$

connected in series. This delivers a power consumption of (ideal circuit)

$$P_{Grid} = 285[V] \cdot 0.350[A] = 99.75[W]$$

due to the fact that the nominal current of the LED is by 350mA. The size of the necessary inductor to limit the current through the LEDs can be calculated with equation 4.12 and results in 2.235H. This means an inductance of 2.235H must be present in each phase of the AC inlet of the B6 bridge. Next the behaviour of the ideal circuit can be calculated with a variable supply voltage. This will show how the ideal three-phase LED lamp will act under service and dimming.

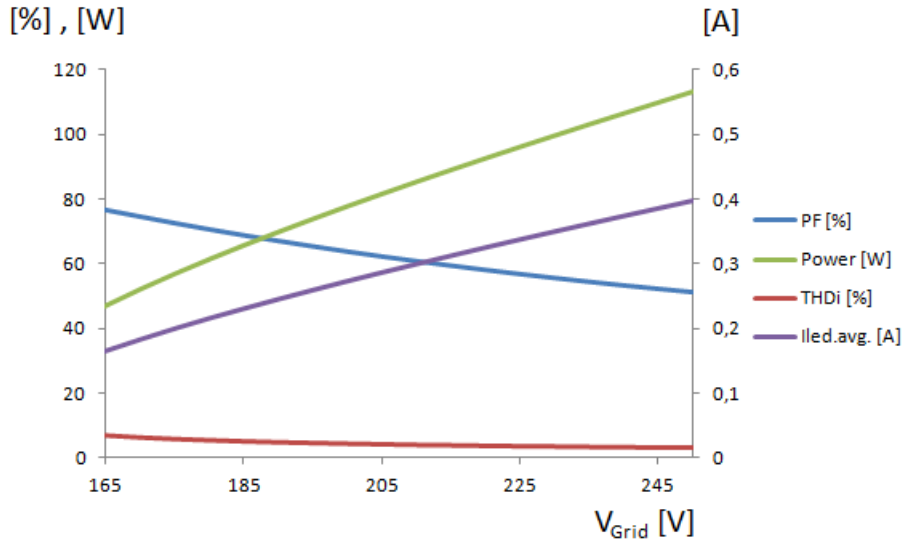

Figure 4.6: Calculation result, $L = 2.235[H], V_{Led} = 285[V]$
PF, THDi, P and $I_{Led.avg.}$ as a function of V_{Grid}

In figure 4.6 the equations B.3.2, B.4.5 and B.5.5 from appendix section B are used for P, THDi and PF respectively. The function for $I_{Led.avg}$ is taken from equation 4.12 above. The value for V_{Grid} is limited for the area 165 - 250V in the diagram. This is done to meet the assumption from section 4.1, which requires that

the phase-to-phase value of the supply voltage must be higher than the V_{Led} value. The value for V_{Grid} has therefore become its limitation in the area:

$$\frac{285}{\sqrt{3}} \; < \; V_{Grid} \; < \; 250 \quad [V]$$

According to figure 4.3 and 4.5 a consideration could be to suggest a value for V_{Led} in the region of 360V. This would theoretically result in a THDi value of 5.1% and a PF of 70% with a inductor of 1.8H, by a limitation of the LED current by 350mA. The result would be a smaller inductor and a better power factor as in the suggested circuit in figure 4.6 with a V_{Led} of 285V. Although this would result in 95 LEDs connected in series and a power consumption of 126W if the same LEDs were used to 350mA.
If the LED voltage of 360V would be adherence and a lower power consumption would be wanted this again would require a larger inductor. The limitation to 250mA LED current would with $V_{Led} = 360V$ require an inductor of 2.5H.

4.4 Simulation of B6 circuit

Pspice again is used to simulate the B6 equivalent circuit given below in figure 4.7. This circuit represents the real circuit in practice with sufficient accuracy. It is the circuit described in the previous section with the 75 LEDs connected in series that is simulated. The simulation is used to examine the circuit when the resistive part is added, and to verify the accuracy of the results from figure 4.6. The chosen 75 LEDs connected in series from previous section deliver according to section 2.5

$$R_{Led} = 2.8[\Omega] \cdot 75 = 210[\Omega] \tag{4.13}$$

The amplitude of V_{Led} according to equation 2.3 in section 2.5 becomes:

$$V_{Led} = 2.82 \cdot 75 \approx 211.5[V] \tag{4.14}$$

The resistive part from the inductance in each phase is for the simulation set to a value of 5Ω. The Pspice simulation circuit with its values is shown in figure 4.7.

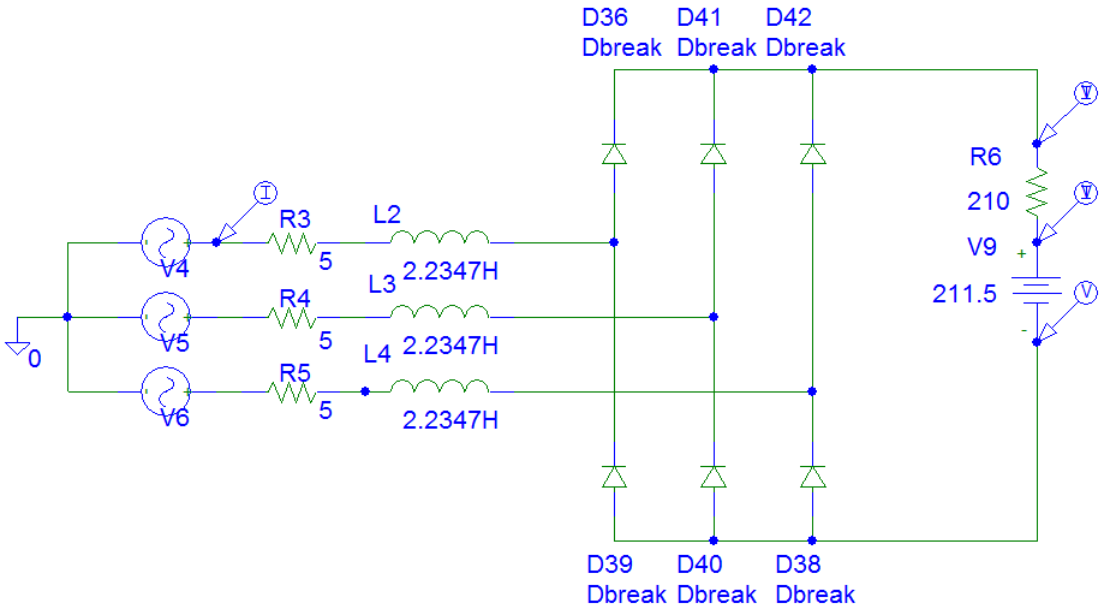

Figure 4.7: Pspice real equivalent circuit used for simulation
$R_L = 5[\Omega], L = 2.2347[H], R_{Led} = 210[\Omega], V_{Led} = 211.5[V]$

The simulation has been carried out in 10V steps. The results are represented in tabular form in figure 4.9. The Fourier analysis is carried out for the current flowing through R3. Again Pspice has been adjusted as described in section 3.4 and the values presented in figure 4.9 have been taken from Pspice in the same way.
Below the results from the simulation is shown. The values are taken from the table in figure 4.9.

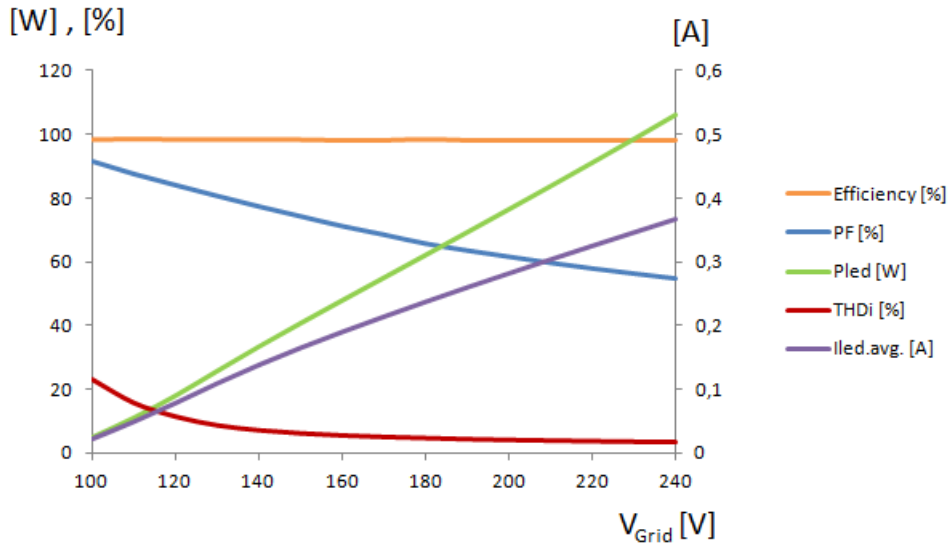

Figure 4.8: Result simulation real equivalent circuit values from figure 4.9

Vgrid [V]	Igrid.rms [mA]	Pgrid [W]	PF [%]	I1.grid [mA]	φ1 [DEG]	THDi [%]	η [%]	Vled.avg [V]	Iled.avg [mA]	Vled.rms [V]	Iled.rms [mA]	Pled [W]
240	273,5	108,058	54,87	387	56,74	3,2	98,4	288,73	367,75	288,77	268,55	106,3
230	258	100,4581	56,43	365	55,66	3,33	98,2	284,33	346,8	284,37	347,5	98,7
220	242,5	92,87463	58,03	342,7	54,5	3,49	98,3	279,9	325,7	279,94	326,35	91,25
210	226,5	85,26626	59,75	320,5	53,33	3,69	98,4	275,38	304,2	275,42	304,87	83,86
200	210,5	77,90756	61,68	297,6	51,9	3,88	98,3	270,8	282,5	270,83	283	76,55
190	194,5	70,52702	63,62	274,4	50,38	4,14	98,3	266,15	260,3	266,18	260,8	69,33
180	177,5	63,02899	65,76	250,5	48,78	4,49	98,6	261,4	237,6	261,42	238,1	62,15
170	160	55,9524	68,57	226,4	46,74	4,84	98,3	256,5	214,3	256,52	214,75	55
160	142,5	48,70576	71,21	201,4	44,56	5,32	98,3	251,44	190,25	251,46	190,7	47,86
150	123,5	41,28655	74,29	174,9	42,11	6	98,5	246,17	165,1	246,18	165,45	40,66
140	104	33,78819	77,35	147	39,29	6,99	98,6	240,57	138,38	240,58	138,7	33,3
130	82,7	26,00557	80,63	116,8	36,16	8,56	98,6	234,45	109,3	234,46	109,55	25,64
120	59,9	18,1131	84	84,49	32,63	11,33	98,5	227,94	78,3	227,94	78,45	17,85
110	38,15	11,01441	87,49	53,44	27,96	15,7	98,7	221,79	49	221,79	49,13	10,87
100	17,4	4,771018	91,4	24,07	20,87	23,17	98,5	216,08	21,8	216,08	21,92	4,7

Figure 4.9: Pspice results from simulation three-phase LED driver figure 4.7
$P_{Grid} = 3 \cdot V_{Grid} \cdot I_{1.Grid} \cdot cos(\phi 1)/\sqrt{2}$, $PF = \frac{P_{Grid}*100}{3 \cdot V_{Grid} \cdot I_{Grid.rms}}$, $\eta = \frac{P_{Led} \cdot 100}{P_{Grid}}$

The trends describe how the three-phase LED lamp acts when the supply voltage is adjusted which equals the situation when the lamp is being dimmed. When the supply voltage is 230V phase-to-neutral the consumed power from the 75 LEDs according to figure 4.9 is approximately 98.7W. Originally the circuit was designed to have a power consumption of 99.75W at 230V, using the ideal circuit without

any resistive components. The difference equates a failure of only 1% in the power consumption. Figure 4.8 also gives the parameters of the circuit in case the phase-to-phase value of the supply voltage is below V_{Led}.

Below in figure 4.10 a snap-shot of the grid current and the bridge AC-input voltage is taken, for a grid supply voltage of 230V. The red trace in the upper diagram represents the current through R3 and the blue trace represents the voltage at the input of the B6 bridge. The voltage signal is measured between ground and the point right from the inductor L2 in figure 4.7. In the lower diagram the frequency spectrum of the grid current is pictured. In the left diagram the ratio between the fundamental frequency at 50Hz to the harmonic distortion is seen. In the right diagram the scale of the current has been zoomed for demonstrating the low current harmonics. Furthermore, it can be observed that only harmonics of order 5, 7, 11, 13,... appear which also was mentioned in the theoretical part in section 4.1.

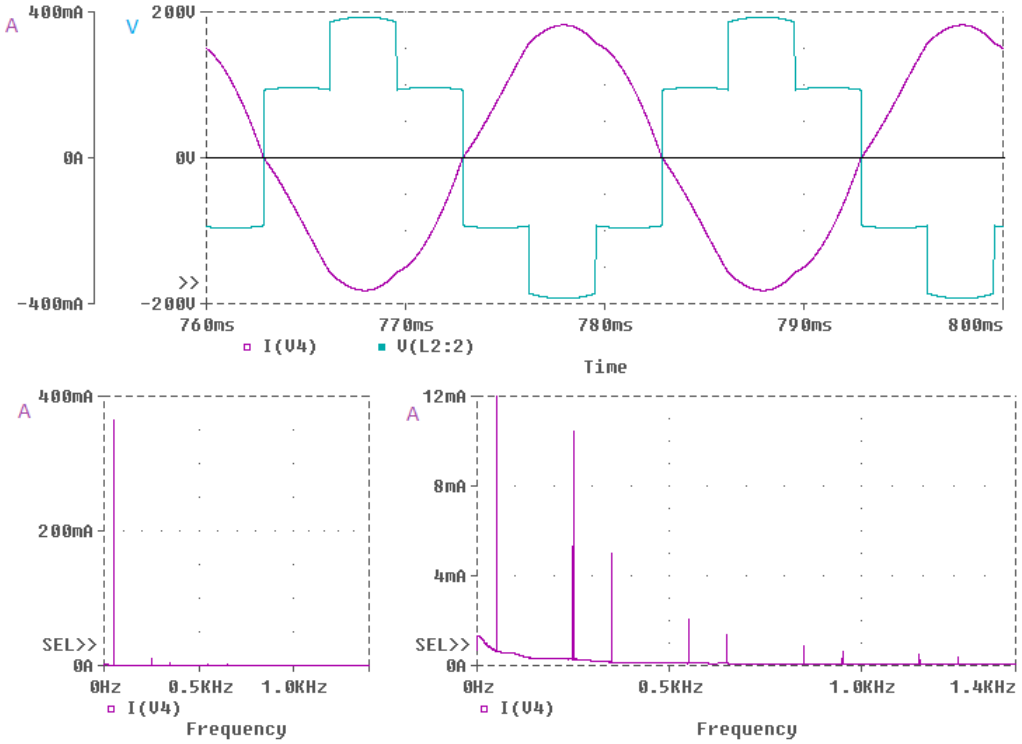

Figure 4.10: Result simulation of figure 4.7 , $V_{Grid} = 230[V]$
Upper diagram: Red(grid current), Blue(Voltage signal inlet B6 bridge)
Bottom: left diagram(FFT grid current), right diagram(zoom FFT grid current)

Figure 4.11 pictures the LED current in connection with the total voltage across the series connection of the LEDs. The supply voltage was here 230V. The current(red trace) refers to the left vertical axis and the voltage drop(blue trace) to the right vertical axis. The LED current ripples only slightly around its average value of 350mA, and the total voltage around 285V.

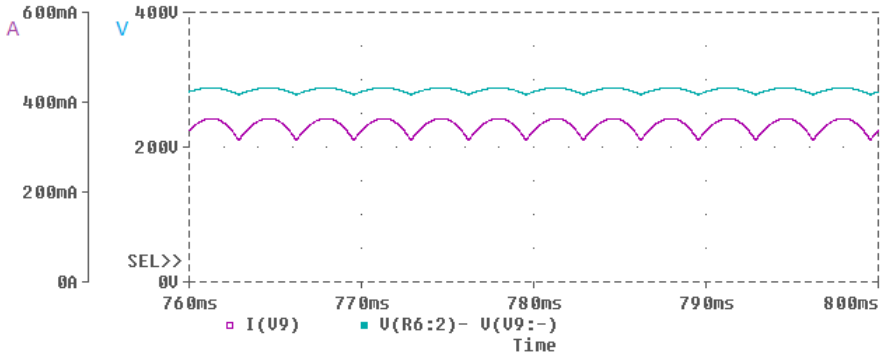

Figure 4.11: Result simulation of figure 4.7, $V_{Grid} = 230[V]$
blue trace(LED current), red trace(voltage drop LEDs)

In figure 4.12 the grid current and the bridge voltage can be observed when the supply voltage is only 120V. Recognizable is that the edge of the bridge input voltage here no longer is a perfect rectangle. This is due to the fact that the phase-to-phase value of the supply voltage is below the sum of the LED voltage drop, which gives a discontinuous grid current as visible in the figure. Further the trace of the supply voltage is added to the diagram(yellow trace). Observable is the phase displacement between current and voltage. If the bridge voltage(blue trace) is subtracted from the supply voltage(yellow trace) further also the integral relation on the grid current can be observed. In the lower diagrams the spectrum of the grid current is given. Visible is the spectrum of the harmonic distortion with the order n=5, 7, 11, 13... which equals f=250Hz, 350Hz, 550Hz, 650Hz...

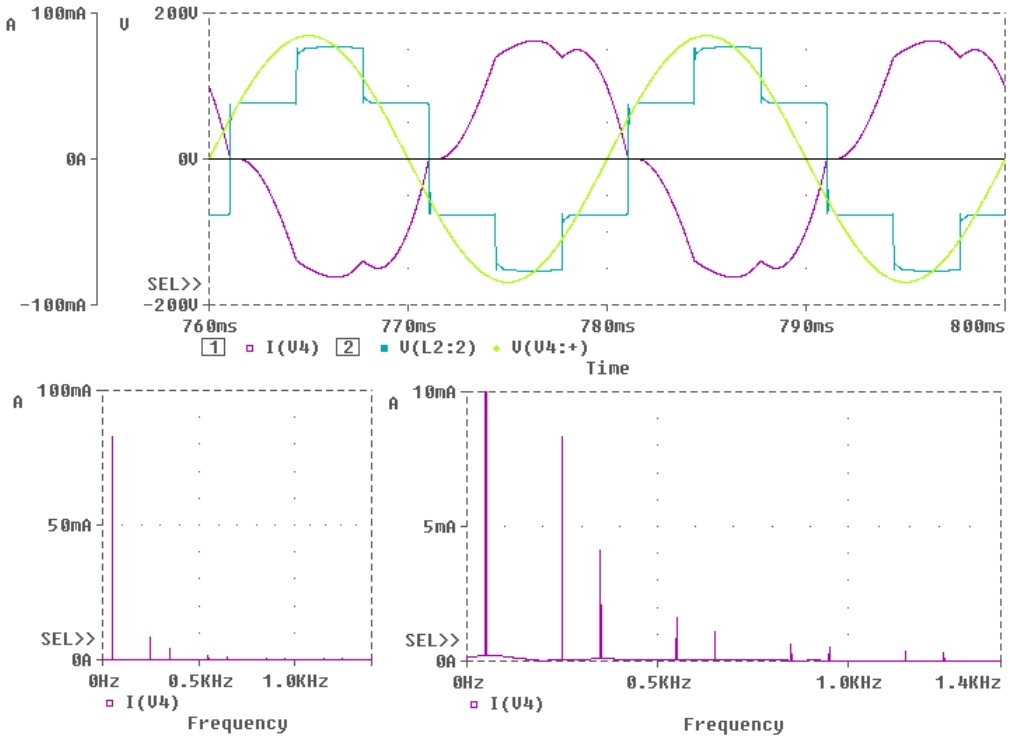

Figure 4.12: Result simulation of figure 4.7, $V_{Grid} = 120[V]$
Upper diagram: Red(grid current), Blue(Voltage signal inlet B6 bridge)
Bottom: left diagram(FFT grid current), right diagram(zoom FFT grid current)

In figure 4.13 the associated LED current is shown together with the total voltage V_{Led} for a supply voltage of 120V. The LED current(blue trace) refers to the left vertical axis and the voltage drop(red trace) refers to the right vertical axis.

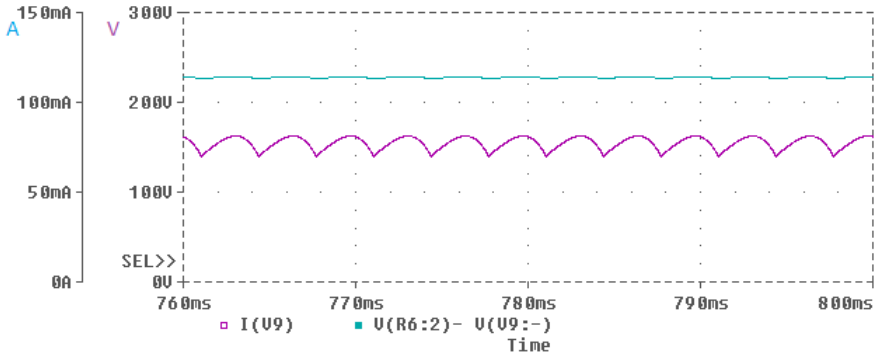

Figure 4.13: Result simulation of figure 4.7, $V_{Grid} = 120[V]$
blue trace(LED current), red trace(total LED voltage)

4.5 Discussion of results - Calculation and simulation

The results of the calculations do correspond very well with the results gained from the simulation. The values for the power factor analog to the single-phase-system are slightly above the values from the calculations due to the added resistance. The THDi value does more or less correspond exactly with the calculated values. In contrast to the single-phase system the three-phase system has a more constant current through the LEDs(compare figure 3.12 and 4.11). This fact results in a more constant voltage across the LEDs like assumed in the calculations of the ideal circuit. The good corresponding THDi values therefore must be the result of this almost constant voltage. The fact that the LED current is continuous is of advantage when stroboscopic effects are considered. The current have a rather low ripple content swinging at 300 Hz.

While taking a closer look into the functions given in figure 4.3 and 4.4 from the calculations a consideration could be to chose a clearly higher V_{Led}. A V_{Led} of 350V would theoretically result, in a PF of 68% and a THDi of 4.8%. If a lamp of 100W is desired the average value of the LED current is to be limited at $100W/350V = 286mA$ which requires an inductor of 2.28H (equation 4.11). The real circuit in practice, with resistive part, would most likely then deliver a PF above 70% at a supply voltage of 230V.

5 Conclusion and discussion

The results of the calculations for the ideal circuits (without resistive part) in figure 3.1 and 4.1 have not differed significantly from the results of the simulated circuits in Pspice, with added resistances (see figure 3.8 and 4.7).
The calculations have shown that the power factor and the value of the total harmonic distortion for the LED lamp mainly depend on how many LEDs are connected in series (see figure 2.3 and 2.4). Put another way, PF and THDi can be specified by the total voltage of all LEDs connected in series. A balance between PF and THDi must be chosen due to the fact that PF and THDi increase when the voltage increases. If the approach for the design of the two LED devices is taken by the inductor size or power consumption, figure 3.5 and 3.6 for the single-phase system, and figure 4.4 and 4.5 for the three-phase system are useful. These figures display the necessary inductance value of the choke depending on how powerful the device shall be. The duty of the inductor is to limit the LED current and hence the power consumption.
An example of a single-phase system was given with 33 white power LEDs and an inductor of 1.5H. This resulted in a power consumption of 47W for the simulated lamp with a power factor of 53.2% and a THDi of 5.5%. An example of a three-phase lamp was studied with 75 power LEDs and a required inductance of 2.23H in each phase. This resulted in a power consumption of 100W with a power factor of 56.43% and a THDi of 3.3%. Constructing lamps with a power consumption lower than 100W, with the three-phase system, requires either an increased inductance value or results in a power factor below 50% according to the calculations.

As has been shown earlier, the simulation basically verifies the calculations. But it is important to keep in mind that the simulated model can or will differ from the values of the real circuit in use. The results taken from the simulation in Pspice (figure 3.9 and 4.8) are both performed with linear inductors. A non-linear inductor will effect the values for THDi and PF. A challenge associated with the two passive LED drivers therefore is the design of the used inductors. Nevertheless heavy saturation of the core from the transient effect when switching on the lamp can be counteracted by using an adjustable voltage supply source (see figure 2.1 and 2.2). The adjustable voltage source offers the possibility to raise the supply voltage slowly. Further, for the calculations and simulation it is assumed that the supply voltage is an ideal sine wave. Harmonics in the supply voltage will contribute to power transmission due to harmonics in the current. This effect should therefore be considered, when overloading is handled.

An interesting feature of the represented passive LED drivers is that the reduction of the LED's voltage by raising service temperature has no negative effect to the system. The advantage results from the fact that the power consumption does not increase when a minor reduction of (V_{Led}) around the operating point takes place. This can be confirmed by derivation of the equations for the power consumption (A.3.2 and B.3.2) around the working point or by a simple numerical example: The LED from section 2.5 change the forward voltage by -2mV/°C in nominal service at 350 mA. Assuming a raise in the operating temperature of 30°C will make the forward voltage drop from 3.8 V to 3.74 V. While considering the single-phase example with 33 LEDs connected in series, the voltage drop V_{Led} will drop from 125.4 to 123.4V. According to equation A.3.2, this will make the power consumption drop from 43.8 to 43.5W ($V_{Grid} = 230V$). The same consideration can be made with the three-phase system consisting of 75 LEDs connected in series from section 4.3. The total LED voltage will decrease from 285V to 280.5V. According to equation B.3.2, this will reduce the power from 99.7W to 98.2 W($V_{Grid} = 230V$). Although both examples are calculated on the basis of the ideal circuit, the characteristic is proved.

Another subject that needs further examination is whether the announced lifetime prediction of the used LEDs still remains valid when they are operated with the presented passive LED drivers. The commonly used method from IESNA for LED lifetime estimation is used against the background of measurements where the LEDs are driven by an almost perfect direct current, with a maximum ripple of 2%. The passive LED drivers discussed here will supply the LEDs with a current, where the ripple content is clearly over 2%.
Lifetime of the used passive LED drivers, which only consist of diodes and a inductor, shall easily approximate or exceed the estimated lifetime of the inserted LEDs. An important factor for the design of the inductor is to achieve low operating temperatures in service. In this context another important advantage must be mentioned: Inductors have the ability to cut-off high peaks in the supply voltage. The inductor will act as a kind of low pass filter which will protect the lamp. In this way the inductor also positively affects the robustness and stability of the system.

References

[1] Cree inc. Xlamp cxa2011 led.

[2] U. S. Department of Energy. Lifetime of white leds, 2006.

[3] Philips Lumileds. Lifetime behavior of led systems white paper wp15 20121218, 2012.

[4] Edgar Dombrowski. *Einführung in die Zuverlässigkeit elektronischer Geräte und Systeme*. AEG-Telefunken, 1970.

[5] Tridonic. Magnetic chokes for fluorescent lamps, 2012.

[6] Lite-On. White power led lopl-e001m.

List of Figures

A Appendix

A.1 Main equations B2 circuit

The following 6 equations come from section 3.1 and are the fundamental equations for the circuit in figure 3.1. With these equations the parameters of the circuit are calculated. V_{Grid} is the effective value of the phase-to-neutral voltage. $V_{1.C}, V_{1.L}$ and $I_{1.Grid}$ are effective values of the fundamental harmonic oscillation.

Relation between current and voltage drop across inductor:

$$V_{1.L} = I_{1.Grid} \cdot \omega L_{Balast} \tag{A.1.1}$$

From Fourier analysis

$$V_{1.C} = \frac{4}{\pi\sqrt{2}} V_{Led} = \frac{\sqrt{8}}{\pi} V_{Led} \tag{A.1.2}$$

From vector diagram figure 3.2

$$V_{1.C} \cdot cos(\alpha) = V_{Grid} - V_{1.L} \cdot sin(\phi_1) \tag{A.1.3}$$

From vector diagram figure 3.2

$$V_{1.C} \cdot sin(\alpha) = V_{1.L} \cdot cos(\phi_1) \tag{A.1.4}$$

From integral relation

$$\alpha = arccos\left(\frac{V_{Led} \cdot \pi}{\sqrt{8} \cdot \hat{V}_{Grid}}\right) \tag{A.1.5}$$

Power consumption

$$P_{Grid} = V_{Grid} \cdot I_{1.Grid} \cdot cos(\phi_1) \tag{A.1.6}$$

A.2 Calculaion grid current B2 circuit

Starting with A.1.4 and reshaping until A.2.1 occurs

$$cos(\phi_1) = \frac{V_{1.C}}{V_{1.L}} \cdot sin(\alpha) \tag{A.1.4}$$

$$\phi_1 = arccos\left(\frac{V_{1.C}}{V_{1.L}} \cdot sin(\alpha)\right)$$

Using the relation $sin(arccos(x)) = \sqrt{1 - x^2}$

$$sin(\phi_1) = sin\left(arccos\left(\frac{V_{1.C}}{V_{1.L}} \cdot sin(\alpha)\right)\right) = \sqrt{\frac{[V_{1.L}^2 - V_{1.C}^2 \cdot sin^2(\alpha)]}{V_{1.L}^2}}$$

$$sin^2(\phi_1) = \frac{1}{V_{1.L}^2}\left(V_{1.L}^2 - \frac{V_{1.C}^2}{2}\left[1 - cos(2\alpha)\right]\right) \tag{A.2.1}$$

Starting with equation A.1.5 and reshaping until A.2.2 occurs

$$cos(2\alpha) = cos\left(2 \cdot arccos\left[\frac{V_{Led} \cdot \pi}{\sqrt{8} \cdot V_{Grid}}\right]\right) \tag{A.1.5}$$

$$cos(2\alpha) = \frac{\pi^2 \cdot V_{Led}^2}{4 \cdot V_{Grid}^2} - 1 \tag{A.2.2}$$

Putting equation A.2.1 and A.2.2 together and reshaping until A.2.3 occurs

$$sin^2(\phi_1) = \frac{1}{V_{1.L}^2}\left(V_{1.L}^2 - \frac{V_{1.C}^2}{2}\left[1 - \frac{\pi^2 \cdot V_{Led}^2}{4 \cdot V_{Grid}^2} + 1\right]\right) \tag{A.2.1 \& A.2.2}$$

$$sin^2(\phi_1) = \frac{1}{V_{1.L}^2}\left(V_{1.L}^2 + V_{1.C}^2\left[\frac{V_{Led}^2 \cdot \pi^2}{V_{Grid}^2 \cdot 8} - 1\right]\right) \tag{A.2.3}$$

Starting with equation A.1.3 and reshaping until A.2.4 occurs

$$V_{Grid} - V_{1.C} \cdot cos(\alpha) = V_{1.L} \cdot sin(\phi_1) \tag{A.1.3}$$

$$(V_{Grid} - V_{1.C} \cdot cos(\alpha))^2 = V_{1.L}^2 \cdot sin^2(\phi_1) \tag{A.2.4}$$

Putting equation A.2.4 , A.2.3 and A.1.2 together and reshaping until A.2.5 occurs.

$$(V_{Grid} - V_{1.C} \cdot cos(\alpha))^2 = V_{1.L}^2 \cdot \frac{1}{V_{1.L}^2} \left(V_{1.L}^2 + V_{1.C}^2 \left[\frac{V_{Led}^2 \cdot \pi^2}{V_{Grid}^2 \cdot 8} - 1 \right] \right) \tag{A.2.4 \& A.2.3 \& A.1.2}$$

$$V_{1.L}^2 = V_{Grid}^2 + V_{Led}^2 \left(\frac{8}{\pi^2} - 2 \right) \tag{A.2.5}$$

Putting A.1.1 into A.2.5 and reshaping until A.2.6 occurs which is the equation for the effective value of the fundamental harmonic of the grid current.

$$I_{1.Grid} \cdot \omega L = \sqrt{V_{Grid} + V_{Led}^2 \left(\frac{8}{\pi^2} - 2 \right)} \tag{A.1.1 \& A.2.5}$$

$$\underline{I_{1.Grid} = \frac{1}{\omega L} \sqrt{V_{Led}^2 \left(\frac{8}{\pi^2} - 2 \right) + V_{Grid}^2}} \tag{A.2.6}$$

A.3 Calculation power B2 circuit

Here the equation for the power consumption is calculated from the main equations.

Starting by putting A.1.4 together with A.1.5

$$cos(\phi_1) = \frac{V_{1.C}}{V_{1.L}} \cdot sin\left(arccos\left(\frac{V_{Led} \cdot \pi}{\sqrt{8} \cdot V_{Grid}}\right)\right) \qquad \text{(A.1.4 \& A.1.5)}$$

Then adding A.1.2 and A.1.1 into the previous equation together with the relation $sin(arccos(x)) = \sqrt{1 - x^2}$

$$cos(\phi_1) = \frac{V_{1.C}}{4 \cdot V_{1.L}} \cdot \sqrt{\frac{16 \cdot V_{Grid}^2 - 2 \cdot \pi^2 \cdot V_{Led}^2}{V_{Grid}^2}} \qquad \text{(\& A.1.2 \& A.1.1)}$$

Here the equation for the phase angle between the supply voltage and the fundamental harmonic of the grid current is expressed.

$$\underline{cos(\phi_1) = \frac{V_{Led}}{\omega L \cdot I_{Grid}} \sqrt{\frac{8}{\pi^2} - \frac{V_{Led}^2}{V_{Grid}^2}}} \qquad \text{(A.3.1)}$$

Putting equation A.3.1 into A.1.6

$$P_{Grid} = \frac{V_{Grid} \cdot V_{Led}}{\omega \cdot \pi \cdot L} \sqrt{8 - \frac{\pi^2 \cdot V_{Led}^2}{V_{Grid}^2}} \qquad \text{(A.1.6 \& A.3.1)}$$

By reshaping the equation for the power consumption can be calculated

$$\underline{P_{Grid} = \frac{V_{Led}}{\omega L} \sqrt{\frac{8}{\pi^2} \cdot V_{Grid}^2 - V_{Led}^2}} \qquad \text{(A.3.2)}$$

A.4 Calculation THDi B2 circuit

Here the equation for the total harmonic distortion in the grid current is calculated.

Definition:

$$THDi = \sqrt{\frac{I_{n.UH}^2}{I_1^2}} = \sqrt{\frac{I_2^2 + I_3^2 + I_4^2 ...}{I_1^2}} \tag{A.4.1}$$

The spectrum of the harmonic oscillations in the voltage signal before the B2 bridge.

$$\hat{V}_{n.UH} = \frac{4 \cdot V_{Led}}{\pi} \cdot \sum_{n=3,5,7...}^{\infty} \frac{1}{n} \tag{A.4.2}$$

The corresponding spectrum of the current before the B2 bridge

$$\hat{I}_{n.UH} = \frac{\hat{V}_{n.UH}}{\omega \cdot nL} = \frac{4 \cdot V_{Led}}{\pi \cdot \omega L} \cdot \sum_{n=3,5,7...}^{\infty} \frac{1}{n^2} \tag{A.4.3}$$

By reshaping A.4.3 the equation below occurs

$$\hat{I^2}_{n.UH} = \frac{16 \cdot V_{Led}^2}{\pi^2 \omega^2 L^2} \cdot \sum_{n=3,5,7...}^{\infty} \frac{1}{n^4}$$

The sum of the series above was solved with the mathematical program MAPLE and results in:

$$\sum_{n=3,5,7...}^{\infty} \frac{1}{n^4} = \sum_{n=3}^{\infty} \frac{1 - (-1)^n}{2 \cdot n^4} = \frac{\pi^4}{96} - 1$$

Putting the result of the sum into A.4.3 results in following equation:

$$\hat{I^2}_{n.UH} = \frac{16 \cdot V_{Led}^2}{\pi^2 \omega^2 L^2} \cdot \left(\frac{\pi^4}{96} - 1 \right) \tag{A.4.4}$$

Putting equation A.4.4 and A.2.6 from previous section into A.4.1

$$THDi = \sqrt{\frac{\frac{16 \cdot V_{Led}^2}{\pi^2 \omega^2 L^2} \cdot \left(\frac{\pi^4}{96} - 1 \right))}{\frac{2}{\omega^2 L^2} \left(V_{Led}^2 \left(\frac{8}{\pi^2} - 2 \right) + V_{Grid}^2 \right)}} \tag{A.4.1 \& A.4.4 \& A.2.6}$$

Following expression for the total harmonic distortion in the grid current occurs.

$$THDi = \sqrt{\frac{V_{Led}^2(\pi^4 - 96)}{12 \cdot \pi^2 \cdot V_{Grid}^2 + V_{Led}^2(96 - 24 \cdot \pi^2)}} \tag{A.4.5}$$

A.5 Calculation power factor B2 circuit

Definition of power factor:

$$PF = \frac{P}{S} = \sqrt{\frac{P^2}{S^2}} \tag{A.5.1}$$

If assumed that the supply voltage is an ideal sine wave, following equation is valid for the apparent power output. Next below, terms for the currents in the parenthesis are calculated. After that S is calculated an thereafter PF.

$$S^2 = V_{Grid}^2 \cdot I_{Grid}^2 = V_{Grid}^2 \left(I_{1.W}^2 + I_{1.R}^2 + I_{n.UH}^2\right) \tag{A.5.2}$$

From the parentheses above the watt component of the current is reshaped with equation A.2.6 from previous section and formed into equation A.5.3

$$I_{1.W}^2 = I_{1.Grid}^2 \cdot cos^2(\phi_1) \tag{A.2.6 \& A.3.1}$$

$$I_{1.W}^2 = \frac{1}{\omega^2 L^2 \cdot \pi^2} \left(8 \cdot V_{Led}^2 - \frac{V_{Led}^4 \cdot \pi^2}{V_{Grid}^2}\right) \tag{A.5.3}$$

Here the reactive component of the current from equation A.5.2 is reshaped with equation A.2.6 and A.3.1 into equation A.5.4

$$I_{1.R}^2 = I_{1.Grid}^2 \cdot sin^2(\phi_1) = I_{1.Grid}^2 \cdot (1 - cos^2(\phi_1)) \tag{A.2.6 \& A.3.1}$$

$$I_{1.R}^2 = \frac{1}{\omega^2 L^2}\left(V_{Grid} - \frac{V_{Led}^2}{V_{Grid}}\right)^2 \tag{A.5.4}$$

The last equation in the parentheses (A.5.2) expresses the harmonic distortion part in the grid current, which already have been derived in section A.4

$$I_{n.UH}^2 = \frac{1}{\omega^2 L^2} \cdot \frac{V_{Led}^2 \cdot 8}{\pi^2}\left(\frac{\pi^4}{96} - 1\right) \tag{A.4.4}$$

Putting A.5.3, A.5.4 and A.4.4 into A.5.2 following equation for the apparent power consumption can be made by reshaping.

$$S^2 = \frac{V_{Grid}^2}{\omega^2 L^2}\left(V_{Grid}^2 + V_{Led}^2\left(\frac{\pi^2 - 24}{12}\right)\right) \qquad \text{(A.5.2 \& A.5.3 \& A.5.4 \& A.4.4)}$$

Putting the equation above into A.5.1 together with the equation for the power consumption P (A.3.2) derived in section A.3 the final equation for the power factor can be expressed in A.5.5.

$$PF = \sqrt{\frac{P^2}{S^2}} = \sqrt{\frac{\frac{V_{Led}^2}{\omega^2 L^2}\left(\frac{8}{\pi^2} \cdot V_{Grid}^2 - V_{Led}^2\right)}{\frac{V_{Grid}^2}{\omega^2 L^2}\left(V_{Grid}^2 + V_{Led}^2\left(\frac{\pi^2 - 24}{12}\right)\right)}} \qquad \text{(\& A.3.2)}$$

$$\underline{PF = \frac{V_{Led}}{V_{Grid}}\sqrt{\frac{96 \cdot V_{Grid}^2 - V_{Led}^2 \cdot 12 \cdot \pi^2}{V_{Grid}^2 \cdot 12 \cdot \pi^2 + V_{Led}^2 \cdot \pi^2(\pi^2 - 24)}}} \tag{A.5.5}$$

B Appendix

B.1 Main equations B6 circuit

The following 6 equations come from section 4.1 and are the fundamental equations for the three-phase system in figure 4.1. With these equations the parameters of the circuit are calculated. V_{Grid} is the effective value of the phase-to-neutral voltage. $V_{1.C}, V_{1.L}$ and $I_{1.Grid}$ are effective values of the fundamental harmonic.

Relation between current and voltage drop across the inductor.

$$V_{1.L} = I_{1.Grid} \cdot \omega L_{Balast} \tag{B.1.1}$$

From Fourier analysis

$$V_{1.C} = \frac{\sqrt{2}}{\pi} V_{Led} \tag{B.1.2}$$

From vector diagram identical to figure 3.2

$$V_{1.C} \cdot cos(\alpha) = V_{Grid} - V_{1.L} \cdot sin(\phi_1) \tag{B.1.3}$$

From vector diagram identical to figure 3.2

$$V_{1.C} \cdot sin(\alpha) = V_{1.L} \cdot cos(\phi_1) \tag{B.1.4}$$

From integral relation

$$\alpha = arccos\left(\frac{V_{Led} \cdot \pi \cdot \sqrt{2}}{9 \cdot V_{Grid}}\right) \tag{B.1.5}$$

Power consumption

$$P_{Grid} = 3 \cdot V_{Grid} \cdot I_{1.Grid} \cdot cos(\phi_1) \tag{B.1.6}$$

B.2 Calculation grid current B6 circuit

Here the equation for the current is calculated.

Starting with B.1.4 and reshaping until B.2.1 occurs using the relation $sin(arccos(x)) = \sqrt{1-x^2}$

$$cos(\phi_1) = \frac{V_{1.C}}{V_{1.L}} \cdot sin(\alpha) \tag{B.1.4}$$

$$\phi_1 = arccos\left(\frac{V_{1.C}}{V_{1.L}} \cdot sin(\alpha)\right)$$

$$sin(\phi_1) = sin\left(arccos\left(\frac{V_{1.C}}{V_{1.L}} \cdot sin(\alpha)\right)\right) = \sqrt{\frac{[V_{1.L}^2 - V_{1.C}^2 \cdot sin^2(\alpha)]}{V_{1.L}^2}}$$

$$sin^2(\phi_1) = \frac{1}{V_{1.L}^2}\left(V_{1.L}^2 - \frac{V_{1.C}^2}{2}\left[1 - cos(2\alpha)\right]\right) \tag{B.2.1}$$

Starting with B.1.5 and reshaping until B.2.2 occurs using the relation $cos(2arccos(x)) = 2x^2 - 1$

$$cos(2\alpha) = cos\left(2 \cdot arccos\left[\frac{V_{Led} \cdot \pi \cdot \sqrt{2}}{9 \cdot V_{Grid}}\right]\right) \tag{B.1.5}$$

$$cos(2\alpha) = \frac{4 \cdot \pi^2 \cdot V_{Led}^2}{81 \cdot V_{Grid}^2} - 1 \tag{B.2.2}$$

Putting B.2.1 and B.2.2 together with B.1.2 and reshaping until B.2.3 occurs

$$sin^2(\phi_1) = \frac{1}{V_{1.L}^2}\left(V_{1.L}^2 - \frac{V_{1.C}^2}{2}\left[1 - \frac{4 \cdot \pi^2 \cdot V_{Led}^2}{81 \cdot V_{Grid}^2} + 1\right]\right) \qquad \text{(B.2.1 \& B.2.2)}$$

$$sin^2(\phi_1) = \frac{1}{V_{1.L}^2}\left(V_{1.L}^2 + V_{1.C}^2\left[\frac{2 \cdot \pi^2 \cdot V_{Led}^2}{81 \cdot V_{Grid}^2} - 1\right]\right) \qquad \text{(\& B.1.2)}$$

$$sin^2(\phi_1) = \frac{1}{V_{1.L}^2}\left(V_{1.L}^2 + \frac{4 \cdot V_{Led}^4}{81 \cdot V_{Grid}^2} - \frac{V_{Led}^2 \cdot 2}{\pi^2}\right) \tag{B.2.3}$$

Starting with B.1.3 and reshaping

$$V_{1.C} \cdot cos(\alpha) = V_{Grid} - V_{1.L} \cdot sin(\phi_1) \tag{B.1.3}$$

Then putting B.1.5 and B.1.2 into B.1.3 and reshaping until B.2.4 occur

$$sin(\phi_1) = \frac{1}{V_{1.L}}(V_{Grid} - V_{1.C} \cdot cos(\alpha)) \qquad \text{(\& B.1.5 \& B.1.2)}$$

$$sin^2(\phi_1) = \frac{1}{V_{1.L}^2}\left(V_{Grid} - \frac{2 \cdot V_{Led}^2}{9 \cdot V_{Grid}}\right)^2 \tag{B.2.4}$$

Then equate B.2.3 and B.2.4 and reshape until B.2.5 occur

$$\frac{1}{V_{1.L}^2}\left(V_{1.L}^2 + \frac{4 \cdot V_{Led}^4}{81 \cdot V_{Grid}^2} - \frac{V_{Led}^2 \cdot 2}{\pi^2}\right) = \frac{1}{V_{1.L}^2}\left(V_{Grid} - \frac{2 \cdot V_{Led}^2}{9 \cdot V_{Grid}}\right)^2 \qquad \text{(B.2.3\& B.2.4)}$$

$$\left(V_{1.L}^2 + \frac{4 \cdot V_{Led}^4}{81 \cdot V_{Grid}^2} - \frac{V_{Led}^2 \cdot 2}{\pi^2}\right) = \left(V_{Grid} - \frac{2 \cdot V_{Led}^2}{9 \cdot V_{Grid}}\right)^2$$

$$V_{1.L} = \sqrt{V_{Led}^2\left(\frac{2}{\pi^2} - \frac{4}{9}\right) + V_{Grid}^2} \tag{B.2.5}$$

Then adding B.1.1 into B.2.5 and reshape until B.2.6 occur. B.2.6 is the equation for the effective value of the first harmonic in the grid current.

$$I_{1.Grid} \cdot \omega L = \sqrt{V_{Led}^2\left(\frac{2}{\pi^2} - \frac{4}{9}\right) + V_{Grid}^2} \qquad \text{(B.2.5 \& B.1.1)}$$

$$\underline{I_{1.Grid} = \frac{1}{\omega \cdot L}\sqrt{V_{Led}^2\left(\frac{2}{\pi^2} - \frac{4}{9}\right) + V_{Grid}^2}} \tag{B.2.6}$$

B.3 Calculation power B6 circuit

Putting equation B.1.4 and B.1.5 together, then adding B.1.2 and B.1.1 below and reshaping until B.3.1 occurs. B.3.1 is the equation for the phase angle between the supply voltage and the first harmonic of the grid current.

$$cos(\phi_1) = \frac{V_{1.C}}{V_{1.L}} \cdot sin\left(arccos\left(\frac{V_{Led} \cdot \pi\sqrt{2}}{9 \cdot V_{Grid}}\right)\right) \qquad \text{(B.1.4 \& B.1.5)}$$

$$cos(\phi_1) = \frac{V_{1.C}}{V_{1.L}} \cdot \sqrt{1 - \frac{2 \cdot \pi^2 \cdot V_{Led}^2}{81 \cdot V_{Grid}^2}} \qquad \text{(\& B.1.2 \& B.1.1)}$$

$$\underline{cos(\phi_1) = \frac{V_{Led}}{\omega L \cdot I_{Grid}} \sqrt{\frac{2}{\pi^2} - \frac{4 \cdot V_{Led}^2}{81 \cdot V_{Grid}^2}}} \qquad \text{(B.3.1)}$$

Below B.3.1 and B.2.6 is put into B.1.6. By reshaping the equation for the power consumption can be made (B.3.2)

$$P_{Grid} = 3 \cdot V_{Grid} \cdot I_{1.Grid} \cdot cos(\phi_1) \qquad \text{(B.1.6)}$$

$$P_{Grid} = \frac{V_{Grid} \cdot V_{Led} \cdot 3}{\omega L} \sqrt{\frac{2}{\pi^2} - \frac{4 \cdot V_{Led}^2}{81 \cdot V_{Grid}^2}} \qquad \text{(B.1.6 \& B.3.1)}$$

$$\underline{P_{Grid} = \frac{V_{Led}}{\omega L} \sqrt{V_{Grid}^2 \cdot \frac{18}{\pi^2} - V_{Led}^2 \cdot \frac{4}{9}}} \qquad \text{(B.3.2)}$$

B.4 Calculation THDi B6 circuit

Here the ratio of the harmonic distortion to the first harmonic of the grid current is calculated(THDi)

$$THDi = \sqrt{\frac{I_{n.UH}^2}{I_1^2}} = \sqrt{\frac{I_2^2 + I_3^2 + I_4^2 ...}{I_1^2}} \tag{B.4.1}$$

The spectrum of the voltage signal before the B6 bridge (figure 4.2)

$$\hat{V}_{n.UH} = \frac{2 \cdot V_{Led}}{\pi} \cdot \sum_{n=5,7,11,13,17,19...}^{\infty} \frac{1}{n} \tag{B.4.2}$$

The corresponding spectrum of the current before the B6 bridge.

$$\hat{I}_{n.UH} = \sum_{n=5,7,11...}^{\infty} \frac{\hat{V}_{n.UH}}{\omega \cdot nL} = \frac{2 \cdot V_{Led}}{\pi \cdot \omega L} \cdot \sum_{n=5,7,11...}^{\infty} \frac{1}{n^2} \tag{B.4.3}$$

The spectrum of the harmonic oscillations in the grid current greater than one.

$$I^2{}_{n.UH} = \frac{2 \cdot V_{Led}^2}{\pi^2 \omega^2 L^2} \cdot \underbrace{\sum_{n=5,7,11...}^{\infty} \frac{1}{n^4}}$$

Below the sum of the series above is expressed with trigonometric functions from the Fourier analysis. The result of the sum was calculated with the mathematical program Mathcad. From now on the result of the sum equals the letter κ

$$\sum_{n=5,7,11...}^{\infty} \frac{1}{n^4} = \underbrace{\sum_{n=5,7,11...}^{\infty} \frac{(1 + cos(\frac{\pi \cdot n}{3}) - cos(\pi \cdot n) - cos(\frac{2\pi \cdot n}{3}))}{3 \cdot n^4}} \approx 215.114 \cdot 10^{-5} = \kappa$$

Solved with Mathcad

$$I_{n.UH}^2 = \frac{2 \cdot V_{Led}^2 \cdot \kappa}{\pi^2 \omega^2 L^2}; \qquad \kappa = 215.114 * 10^{-5} \tag{B.4.4}$$

By putting B.4.4 and B.2.6 into the definition of THDi from above (B.4.1), the equation for THDi can be expressed in B.4.5

$$THDi = \sqrt{\frac{\frac{2 \cdot V_{Led}^2 \cdot \kappa}{\pi^2 \cdot \omega^2 L^2}}{\frac{1}{\omega^2 \cdot L^2}\left(V_{Led}^2\left(\frac{2}{\pi^2} - \frac{4}{9}\right) + V_{Grid}^2\right)}} \qquad \text{(B.4.1 \& B.4.4 \& B.2.6)}$$

$$\underline{THDi = V_{Led}\sqrt{\frac{2 \cdot \kappa}{V_{Led}^2\left(2 - \frac{4\pi^2}{9}\right) + V_{Grid}^2 \cdot \pi^2}};} \qquad \kappa = 215.114 * 10^{-5} \qquad \text{(B.4.5)}$$

B.5 Calculation power factor B6 circuit

Definition of power factor

$$PF = \frac{P}{S} = \sqrt{\frac{P^2}{S^2}} \qquad \text{(B.5.1)}$$

If assumed that the supply voltage is an ideal sine wave, following equation is valid for the apparent power output. Next below, terms for the currents in the parenthesis is calculated. After that S is calculated an thereafter PF.

$$S^2 = 9 \cdot V_{Grid}^2 \cdot I_{Grid}^2 = 9 \cdot V_{Grid}^2\left(I_{1.W}^2 + I_{1.R}^2 + I_{n.UH}^2\right) \qquad \text{(B.5.2)}$$

From the parenthesis above the watt component of the current is together with equation B.2.6 and B.3.1 reshaped into equation B.5.3

$$I_{1.W}^2 = I_{1.Grid}^2 \cdot cos^2(\phi_1) \qquad \text{(B.2.6 \& B.3.1)}$$

$$I_{1.W}^2 = \frac{1}{\omega^2 L^2}\left(V_{Led}^2 \cdot \frac{2}{\pi^2} - \frac{V_{Led}^4 \cdot 4}{V_{Grid}^2 \cdot 81}\right) \qquad \text{(B.5.3)}$$

Here the reactive component of the current from equation B.5.2 above is reshaped with B.2.6 and B.3.1 until B.5.4 occurs

$$I_{1.R}^2 = I_{1.Grid}^2 \cdot sin^2(\phi_1) = I_{1.Grid}^2 \cdot (1 - cos^2(\phi_1)) \qquad \text{(B.2.6 \& B.3.1)}$$

$$I_{1.R}^2 = \frac{1}{\omega^2 L^2}\left(V_{Grid}^2 - V_{Led}^2\frac{4}{9} + \frac{V_{Led}^4 \cdot 4}{V_{Grid}^2 \cdot 81}\right) = \frac{1}{\omega^2 L^2}\left(\frac{9 \cdot V_{Grid}^2 - 2 \cdot V_{Led}^2}{81 \cdot V_{Grid}^2}\right)^2 \qquad \text{(B.5.4)}$$

This equation, derived in section B.4, expresses the upper harmonics in the current greater than one.

$$I_{n.UH}^2 = \frac{2 \cdot V_{Led}^2 \cdot \kappa}{\pi^2 \omega^2 L^2} \qquad \text{(B.4.4)}$$

Finally the apparent power can be calculated by putting B.5.3 , B.5.4 and B.4.4 into equation B.5.2

$$S^2 = \frac{9 \cdot V_{Grid}^2}{\omega^2 L^2}\left(V_{Grid}^2 + V_{Led}^2\left(\frac{18(1+\kappa) - 4 \cdot \pi^2}{9 \cdot \pi^2}\right)\right) \qquad \text{(B.5.2 \& B.5.3 \& B.5.4 \& B.4.4)}$$

After that the apparent power above is put into equation B.5.1 together with the equation for the power consumption derived in section B.3.

$$PF = \sqrt{\frac{P^2}{S^2}} = \sqrt{\frac{\frac{V_{Led}^2}{\omega^2 L^2} \cdot \left(V_{Grid}^2 \cdot \frac{18}{\pi^2} - V_{Led}^2 \cdot \frac{4}{9}\right)}{\frac{9 \cdot V_{Grid}^2}{\omega^2 L^2}\left(V_{Grid}^2 + V_{Led}^2\left(\frac{18(1+\kappa) - 4 \cdot \pi^2}{9 \cdot \pi^2}\right)\right)}} \qquad \text{(\& B.3.2)}$$

Finally the equation for the power factor of the three phase system is expressed in B.5.5

$$\underline{PF = \frac{V_{Led}}{V_{Grid}}\sqrt{\frac{V_{Grid}^2 \cdot 162 - V_{Led}^2 \cdot 4 \cdot \pi^2}{V_{Led}^2(162[1+\kappa] - 36 \cdot \pi^2) + V_{Grid}^2 \cdot 81 \cdot \pi^2}};} \qquad \kappa = 215.114 * 10^{-5} \qquad \text{(B.5.5)}$$

C Appendix

C.1 Simulation B2 circuit

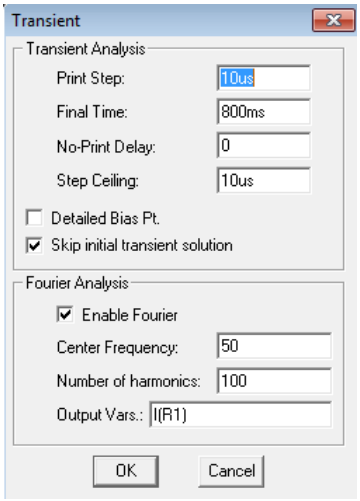

Figure C.1: Setup transient analysis Pspice

FOURIER COMPONENTS OF TRANSIENT RESPONSE I(R_R1)

DC COMPONENT = 7.115407E-05

HARMONIC NO	FREQUENCY (HZ)	FOURIER COMPONENT	NORMALIZED COMPONENT	PHASE (DEG)	NORMALIZED PHASE (DEG)
1	5.000E+01	5.558E-01	1.000E+00	-5.774E+01	0.000E+00
2	1.000E+02	1.219E-04	2.194E-04	-7.725E+01	-1.951E+01
3	1.500E+02	2.840E-02	5.109E-02	-6.071E+01	-2.979E+00
4	2.000E+02	2.535E-05	4.562E-05	-7.011E+01	-1.237E+01
5	2.500E+02	1.022E-02	1.838E-02	-1.653E+02	-1.076E+02
...					
98	4.900E+03	3.276E-07	5.893E-07	2.591E+01	8.365E+01
99	4.950E+03	2.701E-05	4.860E-05	2.539E+01	8.313E+01
100	5.000E+03	3.260E-07	5.866E-07	2.639E+01	8.412E+01

TOTAL HARMONIC DISTORTION = 5.570638E+00 PERCENT

Figure C.2: Output file result analysis of grid current $V_{Grid} = 230[V]$

D Experiment

Laborversuch:
Speisung von Power-LEDs mit konventionellem (magnetischen) Vorschaltgerät

Anordnung:

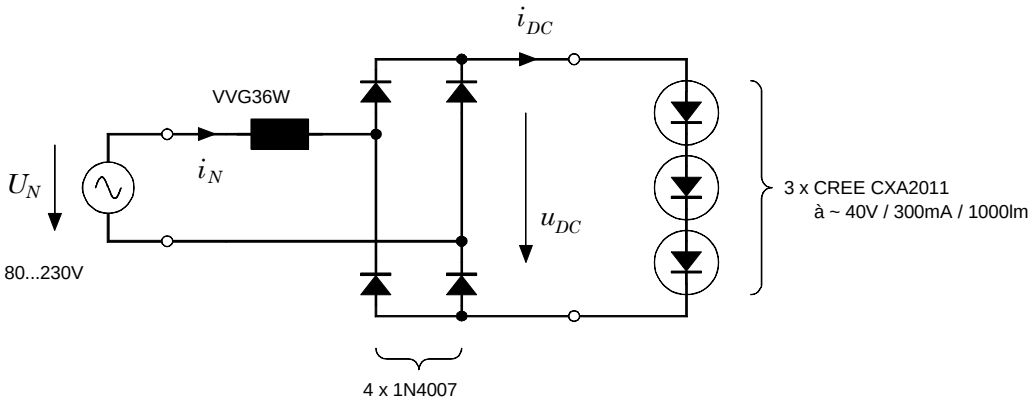

Messergebnisse:

UN (V)	In_rms (mA)	PN (W)	PF	IN_1 (mA)	IN_3 (mA)	IN_5 (mA)	THD IN (%)	a=P_LED/PN	UDCavg (V)	IDCavg (mA)	Urms (V)	Irms (mA)	P_LED (W)	kilo-LUX	T_VVG (°C)
230	403	55,4	0,595	402	36	3,7	9,3	84,47653	127,5	352	127,8	403,3	46,8	16,3	41,7
220	371	50	0,613	368	34	5	9,6	85,4	126,6	323	126,9	371,3	42,7	15,1	
210	341	45,2	0,63	339	33	6	10	86,50442	125,8	299	126,1	343	39,1	14,1	
200	311	40,3	0,65	310	32	7,2	10,7	87,09677	124,9	271	125,1	311	35,1	12,9	
190	279	35,2	0,67	275	32	7,2	11,9	88,35227	123,8	242	124,1	280	31,1	11,7	
180	245	30,3	0,69	243	30	8,4	13,2	88,77888	122,6	212	122,8	246	26,9	10,4	
170	212	25,6	0,71	210	29	8,8	14,8	87,89063	121,2	180	121,4	210	22,5	8,9	26,4
160	180	20,9	0,73	178	29	8,7	17,2	89,47368	119,6	151	119,8	179	18,7	7,6	
150	153	17	0,74	151	28	8,5	19,9	91,76471	117,6	126	117,9	153	15,6	6,4	
140	123	13	0,76	119	26	8,6	23,5	90,76923	114	98	114,7	212,1	11,8	4,9	
130	95,4	9,7	0,78	92,5	24	7,5	27,8	92,78351	109,9	75	111,4	95,3	9	3,9	
120	70	6,7	0,79	66,7	21	5,9	33	92,98507	104,1	53,3	106,8	69,3	6,23	2,7	
110	48,2	4,3	0,81	45	17,3	4	40	94,65116	97,5	35	101,7	48,1	4,07	1,8	
100	28	2,3	0,81	25	12	2,7	50,6	93,04348	88,4	19	95,2	27,8	2,14	0,95	19,2
90	12	0,87	0,78	10	6	2,2	67	96,55172	79,5	7,5	87,6	12,2	0,84	0,36	
80	2,5	0,15	0,7	1,8	1,3	0,8	94		71,4	1,1	79			0,05	

Lux-Meter PAN LX 1308, Abstand LED-Sensor = 27cm, Labor-Umgebungstemperatur ca. 17°C
LEDs: 3x Cree CXA2011 in Serie, Farnell-Best.Nr.: 188 66 90 + 188 66 89 +188 66 84

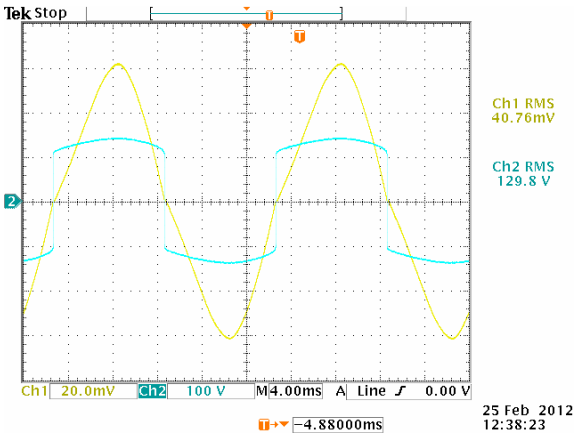

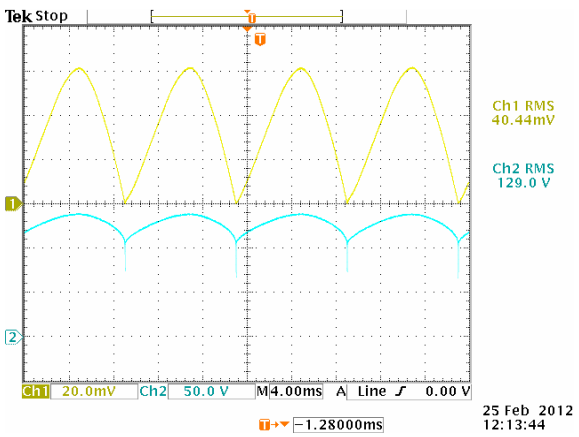

UN=230V: Bild links: Netzstrom (gelb, 200mA/div) und Spannung UX (blau, Gleichrichtereingang, 100V/div); Bild rechts: iDC (gelb, 200mA/div.) uDC (blau, 50V/div).

Bei reduzierten Netzspannungen:

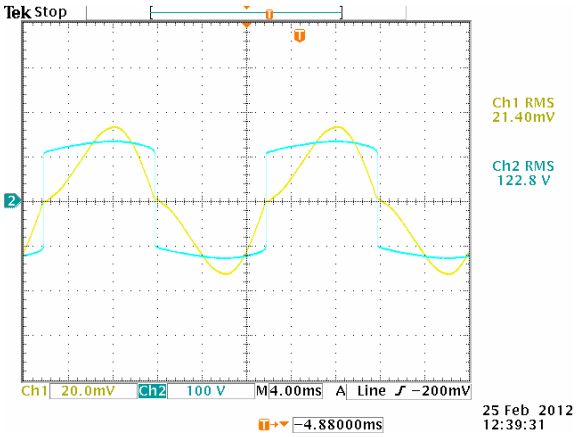

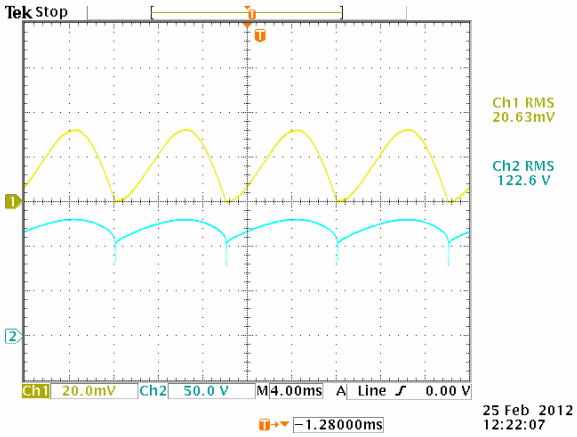

UN=170V

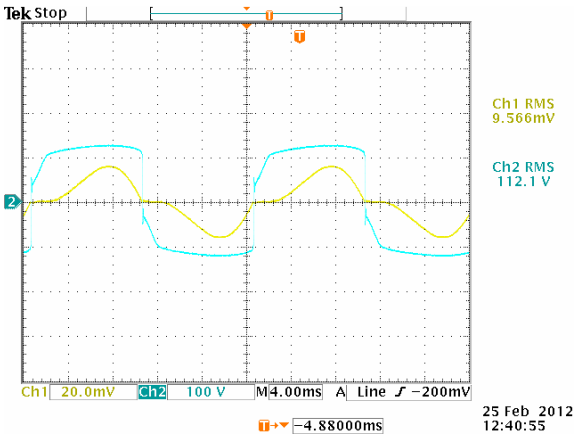

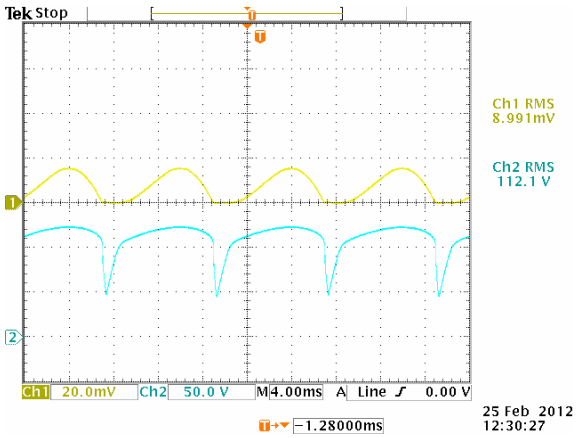

UN=130V

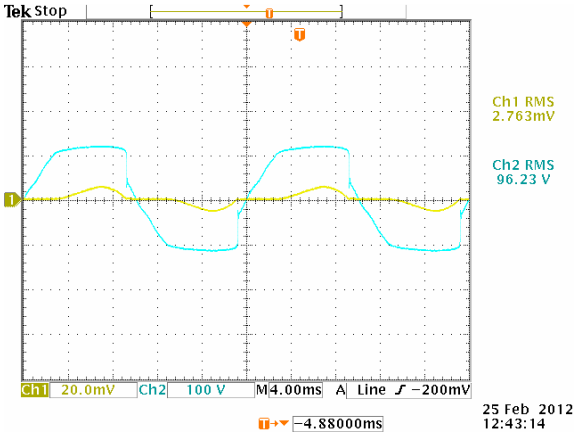

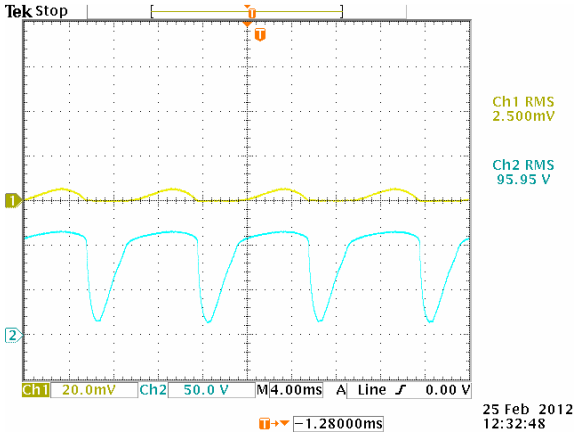

UN=100V

Graphische Darstellung der Meßergebnisse:

Messung von

PN = aufgenommene Wirkleistung aus dem Netz (W)

PLED = an die LED abgegebene mittlere Leistung (W)

ETA = Wirkungsgrad des Vorschaltgerätes = PLED / PN (%)

PF = totaler Leistungsfaktor PN/SN
(nicht nur der $\cos\varphi_1$ der Grundschwingung!)
Könnte mit Parallel-Kompensationskondensator verbessert werden.

THD = Netzstrom-Oberschwingungen (total harmonic distortion) (%)

IN% = Netzstrom-Effektivwert (normiert auf UN = 230V, 405mA)

IDC% = LED-Strom-Mittelwert (normiert auf UN = 230V, 352mA)

kLUX = gemessene Lichtintensität (kilo-Lux)

in Abhängigkeit der Netzspannung (Effektivwert)

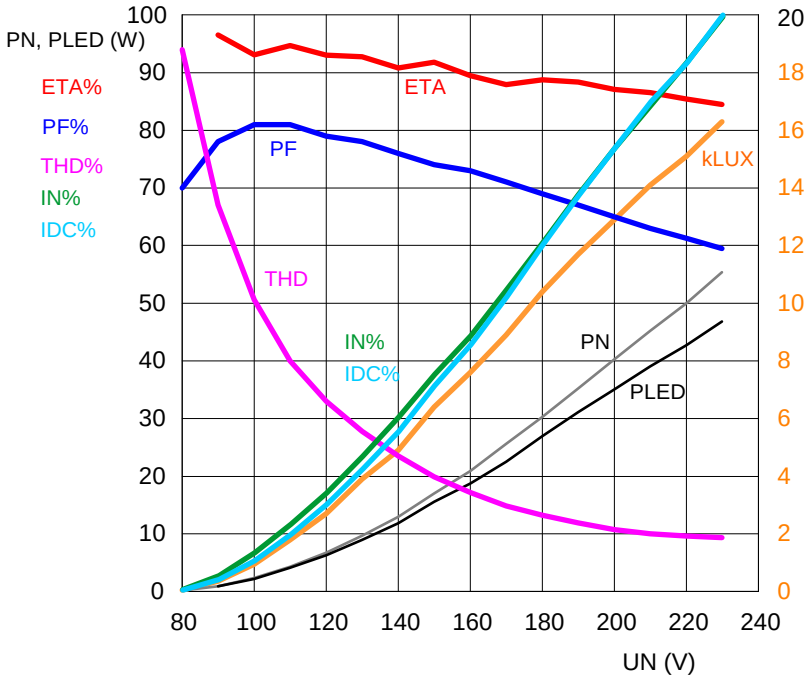

Fotos vom Versuchsaufbau:

Verwendetes Magnetisches Vorschaltgerät VVG36

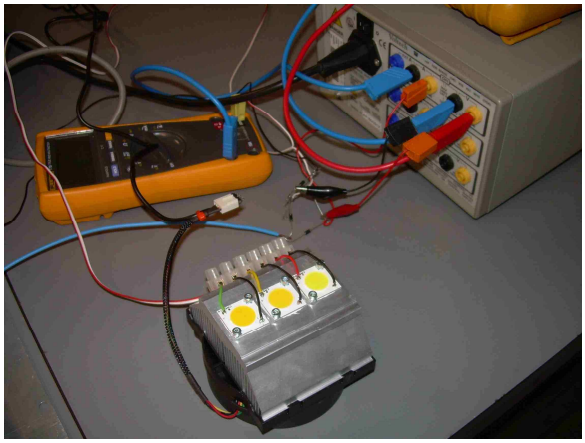
Gleichrichterdioden (Bildmitte)

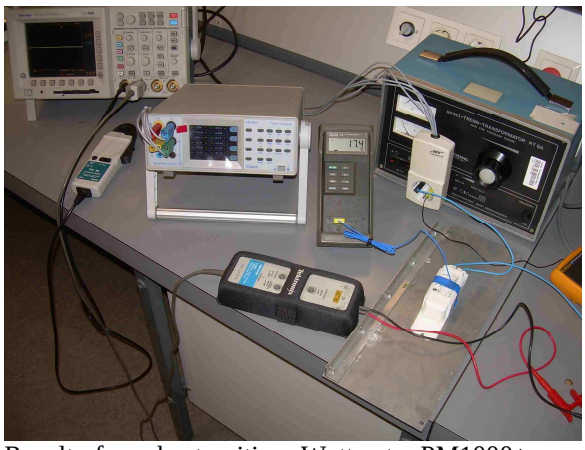
Regeltrafo und netzseitiges Wattmeter PM1000+

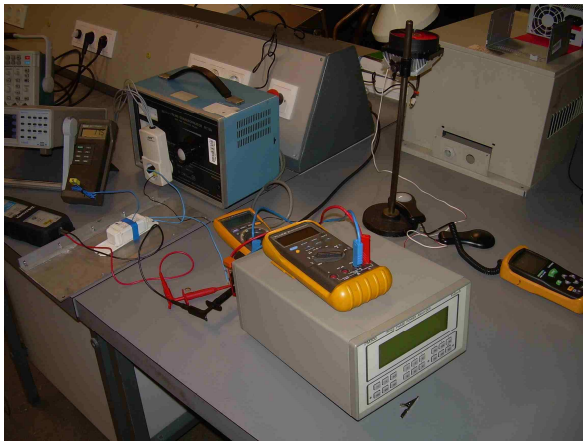
LED-seitiges Wattmeter PM300, LEDs mit Lux-Meter

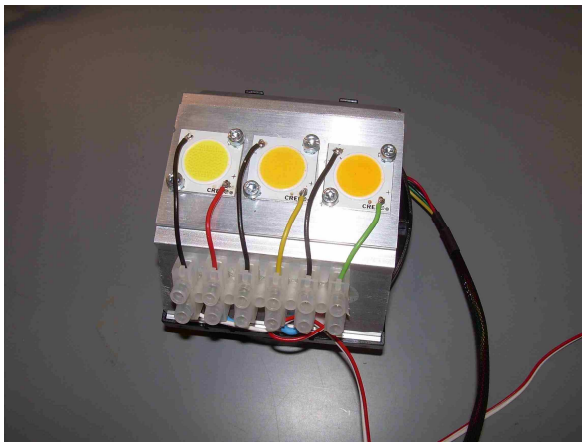
LEDs auf Kühler (3x Cree CXA2011, hier zu Testzwecken mit unterschiedlichen Farbtemperaturen)